Chapter 9

Modelling the Earth's Magnetic Field from Global to Regional Scales

Jean-Jacques Schott and Erwan Thébault

Abstract In the recent years, a large amount of magnetic vector and scalar data have been measured or made available to scientists. They cover different ranges of altitudes from ground to satellite levels and have high horizontal densities over some geographical areas. Processing these potential field data may require alternatives to the widely used Spherical Harmonics. During the past decades, new techniques have been proposed to model regionally the magnetic measurements. They complement the set of older approaches that were revived and sometimes revised in the meantime. The amount of available techniques is intimidating and one often wonders which method is the most appropriate for what purpose. In this paper, we review several modelling strategies. Starting from the Spherical Harmonics, we discuss methods with global support (wavelets, multi-scale, Slepian functions,...) and then bring the focus on regional methods with local support (Rectangular Harmonic Analysis, Cylindrical Harmonic Analysis, Spherical Caps,...). We briefly examine the theoretical aspects and properties of each approach. We compare them with the help of a unique set of perfect synthetic data that mimic an ideal spatial distribution at a fixed surface. This helps us to better emphasize the theoretical characteristics of each approach and suggest, when relevant, improvements that would be useful for future practical applications.

J.-J. Schott (✉)
Ecole et Observatoires des Sciences de la Terre, Université de Strasbourg, F-67084 Strasbourg, France
e-mail: jj.schott@eost.u-strasbg.fr

9.1 Introduction

During the last assembly of the International Association of Geomagnetism and Aeronomy (IAGA) that took place in Sopron, Hungary, and within the division V ("Geomagnetic Observatories, Surveys and Analyses"), a significant number of contributions were related to global and regional modelling of the Earth's magnetic field. The ubiquity of this topic through sessions is a nice tribute paid to recent successful and future satellite missions (Friis-Christensen et al., 2006) and to continuous efforts made by the geomagnetic community towards the acquisition, maintenance, compilation, and fast online availability of magnetic data.

We noticed different modelling strategies among the variety of presentations. A first philosophy relied on the properties of Spherical Harmonics (SH) either by modelling all available data in a grand inversion or by modelling sources separately. The former approach is often referred to as a comprehensive inversion, was initiated decades ago (Sabaka and Baldwin, 1993; Langel et al., 1996), and was later pursued until today by including long series of magnetic observatory and recent satellite measurements (Sabaka et al., 2004). This approach can deal with the coupling between the ionosphere and the magnetosphere (see Sabaka et al., 2009; for instance) and the field does not need to be potential. It is based on the Mie representation well described in Backus et al., (1996; Chapter 5) that is not the scope of the present paper as no regional technique currently consider non potential fields. Other models are comprehensive-like but are based on potential field theory (see Gillet et al., 2010 for a review). Such models like, for instance, CHAOS (Olsen et al.,

M. Mandea, M. Korte (eds.), *Geomagnetic Observations and Models*, IAGA Special Sopron Book Series 5,
DOI 10.1007/978-90-481-9858-0_9,

2006), CHAOS-2 models (Olsen et al., 2009), and GRIMM (Lesur et al., 2008), are all exploiting a selection of recent Ørsted (Olsen et al., 2000) and CHAMP (Reigber et al., 2002) satellite data. They mostly focus on the Earth's core field and have therefore low spatial resolution. Improving the resolution may be achieved by modelling the satellite data sequentially. This approach, traditionally dedicated to the modelling of the lithospheric field, uses stringent data selection and correction (Maus et al., 2008), and is therefore more subjective (see Sabaka and Olsen., 2006 for a formal discussion and Thébault et al., 2010 for some practical implications). Whatever the selected SH modelling approach (comprehensive or sequential), the hundreds of kilometer distance between Low Earth Orbiting satellite and the crustal sources introduce a blurring effect. Thus, an horizontal spatial resolution of about 350 km (about SH degree 130) is probably the maximum achievable with data measured at 350 km altitude by a single satellite. Dense near-surface measurements, on the contrary, are closer to the crustal sources and have kilometric spatial resolution (see the World Digital Magnetic Anomaly Map project—WDMAM, Korhonen et al., 2007). Unfortunately, they are also so unevenly distributed at the Earth's scale that the internal SH Gauss coefficients cannot be estimated readily without data interpolation (Hamoudi et al., 2007; Maus et al., 2007b; Maus et al., 2009). This can only be done at the cost of manufacturing synthetic data and thus, possible wrong wavelengths and artefacts. Would the data be uniformly distributed, the number of required Gauss coefficients to represent the data to their intrinsic resolution would be anyway daunting.

The concept of regional modelling is precisely devoted to process dense sets of data available at different altitudes and to adjust the model to the data resolution; the ulterior motive being often to perform spectral analyses. Some methods were proposed in the past but only since the 1980's with the availability of MAGSAT vector satellite measurements (Langel et al., 1980) are they obeying Laplace equation (Alldredge, 1981). Among them, the first family uses functions with global support on the sphere; they are based on spherical splines (Shure et al., 1982), wavelets (e.g., Holschneider et al., 2003) or other types of localized spherical functions (e.g., Lesur, 2006; Simons et al., 2006). The second family relies on functions with local support. They may rely on a flat Earth approximation like the Rectangular Harmonic Analysis (Alldredge, 1981) and the Cylindrical Harmonic Analysis (Alldredge, 1982) or may consider the spherical curvature of the Earth like the Spherical Cap Harmonics Analysis (SCHA, Haines, 1985a) and its revision (Revised-SCHA, Thébault et al., 2004, for instance). This diversity of techniques is confusing and one often wonders what method is the most appropriate for his purpose. All techniques are obviously not equivalent in practice. They are founded on different theoretical arguments and were often originally derived in a framework far from geomagnetism. They address problems using assumptions with which any new application in geomagnetism must be consistent. We easily understand that modelling data in wide areas does not always bear the flat Earth approximation. Likewise, processing multi-level data with a technique not initially designed to allow upward and downward continuation makes little sense, even though it might give some numerical results. Most of the techniques presented here are in a development stage in the framework of geomagnetism. They currently allow mapping the data with more or less success. We consider that a better knowledge of their mathematical foundations will certainly help developing them towards more geophysical applications related, for instance, to spectral analysis, internal/external field separation and source characterization.

In this paper, we focus on potential field modelling techniques and outline the general theoretical properties of each approach by recalling some of their fundamentals. We begin with some generalities deduced from the Spherical Harmonics and proceed from global to regional scales keeping the same conventions when possible. We emphasize the orthogonality and completeness properties of the methods developed and discuss, when applicable, their relationship with Spherical Harmonics. We provide an example of inverse problem using a set of synthetic data distributed equally over a region at a unique altitude. This helps us to discuss the practical feasibility of the techniques regarding rates of convergence of the solutions and edge effects. However, we should keep in mind that real inverse problems often necessitate subtleties and, sometimes, *had hoc* procedures, regularization, or other kinds of *a priori* information. This requires specific 'know-how' acquired by experience. The examples are thus for illustrative purpose and by

no means aimed at demonstrating the performance of one particular technique. In some examples, the setting of the inverse problem is purposefully designed to enhance a specific weakness or strength and therefore precludes direct figure comparisons between techniques.

9.2 Global Modelling With Spherical Harmonics in a Shell

The Spherical Harmonic (SH) expansion is well known and explained in many papers and books (in particular, we refer to Backus et al., 1996). However, for forthcoming discussions and comparisons with regional modelling methods, we provide a general solution of the Laplace equation in a shell and recap some important properties of SH.

The shell $S(b,c)$ is the open bounded set of $\mathbb{R}^3$ defined by $S(b,c) = \{\mathbf{r} \in \mathbb{R}^3 \mid b < \mid \mathbf{r} \mid < c\}$. Due to the spherical symmetry of the problem and to the shape of the boundaries of the domain, the most appropriate solutions are expressed in spherical coordinates (r, θ, φ). Laplace equation then writes

$$\nabla^2(V) = \frac{1}{r^2}\partial_r\left(r^2\partial_r V\right) + \frac{1}{r^2\sin\theta}\partial_\theta\left(\sin\theta\partial_\theta V\right) + \frac{1}{r^2\sin^2\theta}\partial^2_\varphi V, \tag{9.1}$$

$$= \frac{1}{r^2}\partial_r\left(r^2\partial_r V\right) + \frac{1}{r^2}\nabla^2_S(V) = 0, \tag{9.2}$$

where

$$\nabla^2_S(V) = \frac{1}{\sin\theta}\partial_\theta\left(\sin\theta\partial_\theta V\right) + \frac{1}{\sin^2\theta}\partial^2_{\varphi^2} V, \tag{9.3}$$

is the Beltrami-Laplace operator. The spectral properties of this operator are essential for the functions belonging to the Hilbert space defined on the unit sphere $S(1)$, hence for the solid SH. The solutions of Eq. (9.1) in a ball $0 < \mid r \mid < c$ may be expressed in terms of harmonic homogeneous polynomials, an approach adopted by Backus et al. (1996, Section 3.1). This approach has close connections with rotational symmetries on the sphere and with commutativity properties of a class of differential operators on the sphere. However, we cannot generalize this way of doing to domains with geometry breaking up the rotational symmetry. We therefore prefer to deal with the problem from another viewpoint, which yet remains a standard one (Hobson, 1965).

9.2.1 Resolution of Laplace Equation by the Fourier Decomposition Method

In the geocentric reference frame, the Fourier method provides solutions of Eq. (9.1) in terms of products of separate functions of r, θ and φ. This requires setting two Sturm-Liouville problems and one ordinary differential equation. Writing

$$V(r,\theta,\varphi) = R(r)P(\theta)F(\varphi), \tag{9.4}$$

we obtain the following equations

$$d_r\left(r^2 d_r R\right) = \nu(\nu+1)R, \tag{9.5}$$

$$d^2_{\varphi^2} F = -\kappa F, \tag{9.6}$$

Eq. (9.6) being associated to the boundary conditions

$$F(0) = F(2\pi);\ \left(d_\varphi F\right)_0 = \left(d_\varphi F\right)_{2\pi}, \tag{9.7}$$

$$d_u\left[\left(1-u^2\right)d_u P\right] + \left[\nu\left(\nu+1\right) - \frac{\kappa}{1-u^2}\right]P = 0, \tag{9.8}$$

and Eq. (9.8) associated to the boundary conditions

$$P \text{ and } d_u P \text{ finite } at\ 0 \text{ and } \pi, \tag{9.9}$$

with $u = \cos\theta$. Equation (9.5) is an Euler equation of degree 2 without boundary condition. The constant is written $\nu(\nu+1)$ for well-known convenience. At this stage, ν could be real or complex. The differential equation has two independent solutions admissible in the range $[b,c]$

$$R(r) = r^\nu;\ R(r) = r^{-\nu-1}. \tag{9.10}$$

Equation (9.6) is a regular Sturm-Liouville problem with periodic boundary conditions (Eq. 9.7), which dictate the range of values κ and impose them to be

of the form $\kappa = m^2, m \in \mathbb{Z}$. One may take m as a positive or null integer without loss of generality. Thus, Eq. (9.6) has two independent solutions

$$F(\varphi) = e^{im\varphi};\ F(\varphi) = e^{-im\varphi}. \tag{9.11}$$

Note that $F(\varphi)$ is an eigenvector of the operator $-d^2_{\varphi^2}F$ applied to functions belonging to the space $C^2([0, 2\pi]) \cap L^2([0, 2\pi])$, $L^2([0, 2\pi])$ being endowed with the inner product

$$\langle F, G\rangle = \int_0^{2\pi} F(\varphi)\ \overline{G(\varphi)}\ d\varphi. \tag{9.12}$$

On the subspace of the functions verifying Eq. (9.7), $-d^2_{\varphi^2}F$ is self-adjoint. Hence, the eigenvectors $F(\varphi)$ given by Eq. (9.11) are orthogonal. The Sturm-Liouville problem defined by Eqs. (9.8) and (9.9) is termed 'singular' due to the vanishing of the coefficient of the highest derivative order occurring at both ends of the interval. Replacing κ with m^2, and making the successive changes $P(u) = \left(1-u^2\right)^{m/2} T(u)$, $s = (1-u)/2$, the differential Eq. (9.8) is reshaped into an hypergeometric equation

$$\begin{aligned} &s\,(1-s)\,d^2_{s^2}T + (m+1)\,(1-2s)\,d_sT \\ &\quad + (\nu - m)\,(\nu + m + 1)\,T = 0, \end{aligned} \tag{9.13}$$

which solutions have properties described for instance in Morse and Feshbach (1953, Section 5.2). There is only one analytical solution in the vicinity of each singular point ($s = 0$ or 1) and the solution is analytical at both ends if and only if ν is an integer l. This implies that $-l \leqslant m \leqslant l$ and $T(s)$ being a polynomial of degree $l - m$.

Turning back to $P(u)$, it may be shown (for instance, Olver, 1997, p.180) that if l and m are integers, $P(u)$ takes the familiar form derived from Rodrigues's formula and is called associated Legendre functions $P_l^m(\cos\theta)$. Eq. (9.8) may now be written

$$-d_u\left[\left(1-u^2\right)d_uP_l^m\right] + \frac{m^2}{1-u^2}P_l^m = l(l+1)P_l^m, \tag{9.14}$$

which shows that $P_l^m(u)$ is an eigenvector of the operator

$$D_m = -d_u\left[\left(1-u^2\right)d_u\right] + \frac{m^2}{1-u^2}I, \tag{9.15}$$

where I is the identity operator. D_m is self-adjoint on the subspace of the functions belonging to the space $C^2([-1, 1]) \cap L^2([-1, 1])$ and taking finite values at $|u| = 1$, the Hilbert space $L^2([-1, 1])$ being equipped with the inner product $\int f, g\rangle = \int_{-1}^{1} f(u)g(u)du$, with respect to which the Legendre associated functions are orthogonal. Together with the orthogonality properties of the functions $F(\varphi)$ (Eq. 9.11), the orthogonality of P_l^m is a fundamental property of the spherical harmonic expansions. Consider now the space $L^2(S(\rho))$ of the functions defined on the sphere $S(\rho)$ centered on the origin, with radius ρ. $L^2(S(\rho))$ is a Hilbert space for the inner product

$$\langle f, g\rangle = \frac{1}{4\pi}\int_0^{\pi}\int_0^{2\pi} f(\rho,\theta,\varphi)\ \overline{g\,(\rho,\theta,\varphi)}\,\sin\theta\, d\theta\, d\varphi. \tag{9.16}$$

The operator ∇^2_S (Eq. 9.3) is self-adjoint on the subspace $C^2(S(1)) \cap L^2(S(1))$ of the functions taking finite values at $\theta = 0$ and $\theta = \pi$. From the properties of $F(\varphi)$ and $P_l^m(\cos\theta)$ we derive readily that

$$\beta_l^m(\theta,\varphi) = P_l^m(\cos\theta)e^{im\varphi}\ (m = -l, \ldots, l), \tag{9.17}$$

are eigenfunctions of $-\nabla^2_S$ associated to the eigenvalues $l(l+1)$. Thus, to the eigenvalue $l(l+1)$ is associated an eigensubspace of dimension $2l+1$. The functions $\beta_l^m(\theta,\varphi)$ are orthogonal with respect to the inner product defined on $L^2(S(1))$. This property is a straightforward consequence of the orthogonality properties of $F(\varphi)$ and P_l^m. In Geomagnetism, the common convention is to use the Schmidt functions written p_l^m (see Langel, 1987, p. 254 for a definition). However, the norm of the SH $\left\|\beta_l^m\right\|_{L^2(S(1))}$ may take various expressions (see Langel, 1987, p. 255 for the most common ones). The final solutions of the Laplace equation are, according to the Fourier decomposition

$$\psi^m_{i,l}(r,\theta,\varphi) = R_E\left(\frac{R_E}{r}\right)^{l+1}\beta_l^m, \tag{9.18a}$$

$$\psi^m_{e,\,l}(r,\theta,\varphi) = R_E \left(\frac{r}{R_E}\right)^l \beta^m_l, \tag{9.18b}$$

where R_E is the mean earths' radius. Its incorporation in expressions (9.18) is common in earth's magnetic field modelling and traces back at least to Chapman and Bartels (1940). The subscripts '*i*' (inner) and '*e*' (external) are self-explanatory for readers familiar with SH.

9.2.2 Orthogonality and Completeness Properties

The Laplace equation is the most famous example of second-order partial differential equations. In modern studies of second-order PDE in an open set Ω, an extensive use is made of the Sobolev space $H^1(\Omega)$. It is the space of functions belonging to $L^2(\Omega)$ as well as their first derivatives. $H^1(\Omega)$ is a Hilbert space for the inner product $\langle f, g\rangle_{H^1} = \int_\Omega \left[f(\mathbf{r})\overline{g(\mathbf{r})} + \overrightarrow{\nabla}(f(\mathbf{r})) \cdot \overrightarrow{\nabla}(\overline{g(\mathbf{r})})\right] d\tau$ (Reddy, 1998, p. 227). Let be $\Omega = S(b,c)$, and $\partial\Omega$ its boundary: $\partial\Omega = S(b) \cup S(c)$. It may be shown that the functions $\psi^m_{i,l}$ and $\psi^{m'}_{e,l'}$,which belong to $H^1(\Omega)$) are orthogonal with respect to the inner product $\langle .,. \rangle_{H^1}$ unless $l = l'$ and $m = m'$. However, within the frame of the earth's magnetic field modelling, $H^1(\Omega)$ is not the most relevant space because the measured data is the gradient of the potential, not the potential itself. Beside $H^1(\Omega)$, $H^1_0(\Omega)$ which is the subspace of $H^1(\Omega)$ of the functions taking the value 0 on the boundary $\partial\Omega$, is another Sobolev space that plays a prominent role. $H^1_0(\Omega)$ is a closed subspace of $H^1(\Omega)$ with respect to the inner product

$$\langle f, g\rangle_{H^1_0} = \int_\Omega \overrightarrow{\nabla}(f(\mathbf{r})) \cdot \overrightarrow{\nabla}(\overline{g(\mathbf{r})}) d\tau. \tag{9.19}$$

This inner product defines a true norm on $H^1_0(\Omega)$ because $\|f\|_{H^1_0} = 0$ implies $f = 0$ due to the boundary condition. However, $H^1_0(\Omega)$ is still unsuitable in the case of harmonic functions because $\nabla^2(f) = 0$, associated with the condition $f = 0$ on $\partial\Omega$, is an homogeneous Dirichlet problem which unique solution is $f = 0$. It is important, however, regarding the uniqueness of the inverse problem, to find a subspace where Eq. (9.19) provides a true norm. Backus (1986), showed that the scalar magnetic potential V could be chosen such that $\langle V\rangle_r = 0$ without loss of generality, where $\langle V\rangle_r$ stands for the mean value of V on any sphere of radius r ($b < r < c$). Let thus $U(\Omega)$ be the subset of $H^1(\Omega)$ of the functions verifying the property $\langle f\rangle_r = 0$. $U(\Omega)$ is evidently a subspace of $H^1(\Omega)$. In order to avoid confusions, we will note $\langle f, g\rangle_U$ the inner product defined by Eq. (9.19) when it applies to functions belonging to $U(\Omega)$. This inner product defines a true norm on $U(\Omega)$ because if $\|f\|_U = 0$ then $f =$ constant on $U(\Omega)$ but since $\langle f\rangle_r = 0$, then $f = 0$. Backus et al. (1996, p. 125) showed that $\psi^m_{i,l}(r,\theta,\varphi)$ and $\psi^m_{e,l}(r,\theta,\varphi)$ belong to $U(\Omega)$ except for $l = 0$, though for two different reasons. These basis functions are therefore excluded hereafter.

Furthermore, it may be shown that $\psi^m_{i,l}(r,\theta,\varphi)$ and $\psi^m_{e,l}(r,\theta,\varphi)$ are orthogonal with respect to the inner product $\langle .,. \rangle_U$, which means that

$$\left\langle \psi^m_{i,l}, \psi^{m'}_{e,l'} \right\rangle_U = \int_\Omega \overrightarrow{\nabla}(\psi^m_{i,l}(\mathbf{r})) \cdot \overrightarrow{\nabla}(\overline{\psi^{m'}_{e,l'}(\mathbf{r})}) d\tau = 0, \tag{9.20}$$

and

$$\left\langle \psi^m_{i,l}, \psi^{m'}_{i,l'} \right\rangle_U \text{ or } \left\langle \psi^m_{e,l}, \psi^{m'}_{e,l'} \right\rangle_U = 0 \text{ if } l \neq l' \text{ or } m \neq m'. \tag{9.21}$$

Then, using definitions (9.18)

$$\left\|\psi^m_{i,l}\right\|^2_U = \int_\Omega \left|\overrightarrow{\nabla}\psi^m_{i,l}\right|^2 d\tau = 4\pi R_E^3 (l+1) \left[\left(\frac{R_E}{b}\right)^{2l+1} - \left(\frac{R_E}{c}\right)^{2l+1}\right] \left\|\beta^m_l\right\|^2_{S(1)}, \tag{9.22}$$

and

$$\left\|\psi^m_{e,l}\right\|^2_U = \int_\Omega \left|\overrightarrow{\nabla}\psi^m_{e,l}\right|^2 d\tau = 4\pi R_E^3 l \left[\left(\frac{c}{R_E}\right)^{2l+1} - \left(\frac{b}{R_E}\right)^{2l+1}\right] \left\|\beta^m_l\right\|^2_{S(1)}, \tag{9.23}$$

where $\|.\|_{S(1)}$ is the norm defined previously on the Hilbert space $L^2(S(1))$. At last, the question arises of

this set being a base on $U(\Omega)$. If so, only the null function is orthogonal to $\psi_{i,l}^m$ or $\psi_{e,l'}^{m'}$. An elementary proof of this property may be given thanks to the following Green identity (for instance, Reddy, 1998, p. 219)

$$\int_\Omega f\nabla^2\overline{h}d\tau = \int_{\partial\Omega} f\frac{\partial\overline{h}}{\partial n}ds - \int_\Omega \overrightarrow{\nabla}f\cdot\overrightarrow{\nabla}\overline{h}d\tau = \int_{\partial\Omega} f\frac{\partial\overline{h}}{\partial n}ds - \langle f,h\rangle_U, \tag{9.24}$$

where n is the outward unit vector, orthogonal to the boundary. Let f be an harmonic function belonging to $U(\Omega)$. With $h=\psi_{i,l}^m$, Eq. (9.24) becomes

$$\left\langle f,\psi_{i,l}^m\right\rangle_U = (l+1)\left[b^2\left(\frac{R_E}{b}\right)^{l+2}\int_{S(1)} f(b,\theta,\varphi)\overline{\beta}_l^m d\sigma - c^2\left(\frac{R_E}{c}\right)^{l+2}\int_{S(1)} f(c,\theta,\varphi)\overline{\beta}_l^m d\sigma\right], \tag{9.25}$$

and with $h=\psi_{e,l}^m$

$$\left\langle f,\psi_{e,l}^m\right\rangle_U = l\left[c^2\left(\frac{c}{R_E}\right)^{l-1}\int_{S(1)} f(c,\theta,\varphi)\overline{\beta}_l^m d\sigma - b^2\left(\frac{b}{R_E}\right)^{n-1}\int_{S(1)} f(b,\theta,\varphi)\overline{\beta}_l^m d\sigma\right]. \tag{9.26}$$

The unique solution to the system of equations $<f,\psi_{i,l}^m>_U = <f,\psi_{e,l}^m>_U = 0$ is

$$\int_{S(1)} f(b,\theta,\varphi)\overline{\beta}_l^m d\sigma = \int_{S(1)} f(c,\theta,\varphi)\overline{\beta}_l^m d\sigma = 0. \tag{9.27}$$

Since $\left\{\beta_l^m\right\}$ is an orthonormal base on $L^2(S(1))$ (Backus et al, 1996), f is null on the boundary $\partial\Omega$ and since the function f is the solution of the following Dirichlet problem: $\nabla^2(f)=0$ on Ω, $f=0$ on $\partial\Omega$, the unique solution is $f=0$ on Ω.

9.2.3 Spherical Harmonic Expansion and Convergence Properties

Consider now a potential V belonging to $U(\Omega)$. Its SH expansion, S_V, on the basis $\{\psi_{i,l}^m,\psi_{e,l}^m\}$ is the double series

$$S_V = \sum_{l=1}^{\infty}\sum_{m=-n}^{n}\left(g_n^m\psi_{i,l}^m + q_n^m\psi_{e,l}^m\right). \tag{9.28}$$

The internal and external Gauss coefficients g_l^m and q_l^m are respectively given by the relations

$$g_l^m = \frac{1}{\left\|\psi_{i,l}^m\right\|_U^2} < V,\psi_{i,l}^m >_U, \tag{9.29}$$

$$q_l^m = \frac{1}{\left\|\psi_{e,l}^m\right\|_U^2} < V,\psi_{e,l}^m >_U. \tag{9.30}$$

The Green's identity (9.24) may be used to compute the Gauss coefficients in two other ways, which are equivalent to solving a Dirichlet or a Neumann boundary value problem, but give nevertheless the same expression of Gauss coefficients. In geomagnetism and potential theory, V is an harmonic function on Ω, which gradient $\overrightarrow{B} = -\overrightarrow{\nabla}V$ is known on Ω. A standard way of solving this problem is to search for the Gauss coefficients of the SH expansion S_V of V, which minimize the functional

$$d^2 = \int_\Omega \left|\overrightarrow{\nabla}S_V - \overrightarrow{B}\right|^2 d\tau = \langle S_V,V\rangle_U. \tag{9.31}$$

This problem is closely connected to the inverse problem based on the least squares method, which is widely used in geomagnetic field modelling. The functional d^2 is a quadratic form in the Gauss coefficients and it turns out that the coefficients which minimize d^2 are given by Eq. (9.29) and (9.30). Thus, the mean-square solution is the same as the solution of the Dirichlet problem and the Neumann problem. The equivalence between Dirichlet and Neumann problems is specific to the space $U(\Omega)$ but the equivalence between the Dirichlet problem and the minimization of the functional d^2 (Eq. 9.31) is a general property in $H^1(\Omega)$ (Dautray and Lions, 1987, vol. II, p. 632).

We thus now examine the convergence properties of expansion (9.28). From the property of the

set $\{\psi_{i,l}^{m}, \psi_{e,l'}^{m'}\}$ (Eq. 9.18) being a basis of the space $U(\Omega)$, the SH expansion (9.28) converges towards V with respect to the norm $\|\cdot\|_U$. Such convergence is consistent with the least-squares minimization problem set in Eq. 9.31 but does not preclude the Gibbs phenomenon. This typical well-known approximation error occurs in Fourier-like expansions and its quantitative description refers to uniform convergence, which is the convergence associated to the infinity or Chebyshev norm $\|f\|_\infty = \sup|f|$ or $\|f\|_\infty = \sup\left|\overrightarrow{\nabla} f\right|$ on Ω. These norms (or semi-norm regarding the second expression) are typical for spaces of continuous or continuously differentiable functions. The relationship between these spaces and $H^1(\Omega)$ or $U(\Omega)$, and hence between $\|\cdot\|_\infty$ and $\|\cdot\|_U$, is not obvious. Harnack's first theorem on uniform convergence (Kellog, 1929, p. 248) enunciates a condition relevant for the earth's magnetic field modelling, which states that the infinite series S_V converges uniformly towards V if $\overrightarrow{\nabla}_s V$ (the surface gradient, see, for instance, Backus et al., 1996 p. 324) is continuous on the sphere or, in the present case, on the set of two concentric spheres. Thus, in practice, the SH expansion is uniformly convergent if we exclude singular sources on the boundary of the domain of interest, which explains why, to our knowledge, Gibbs phenomenon has not been reported in SH but in very few cases for which a small number of outliers precisely behaved like singular sources on the sphere (e.g., Hamoudi et al., 2007 Section 4.6).

For the following discussions, we construct a benchmark magnetic field over Western Europe. We use the SH models associated to published Gauss coefficients to synthesize a set of perfect data for X, Y and Z magnetic field components. In Fig. 9.1 we present the Z component that results from the superimposition of the main field at epoch 2010 (IGRF11 model, see http://www.ngdc.noaa.gov/IAGA/vmod/igrf.html for details) and an estimation of the crustal field up to SH degree 720 (i.e., a maximum spatial resolution of about 55 km; see Maus, 2010 for details). We call it Z_{all} in the following.

9.3 Other Modelling at a Global Scale

Spherical harmonic expansions remain the fundamental tool for modelling the Earth's magnetic field thanks to their completeness and convergence properties, be it through the Gauss or the Mie representation. Both rely strongly on Newtonian potentials, which verify the Laplace equation in any source-free domain. However, invoking concepts more familiar in the physics of wave propagation and signal processing, some authors argue that there is no possible balance between spectral and spatial localization with SH (e.g., Freeden and Michel, 2000; Lesur, 2006; Simons et al., 2006). SH are indeed perfectly localized in the frequency domain but not localized in space, their support being the whole sphere, and the necessary truncation of the expansion

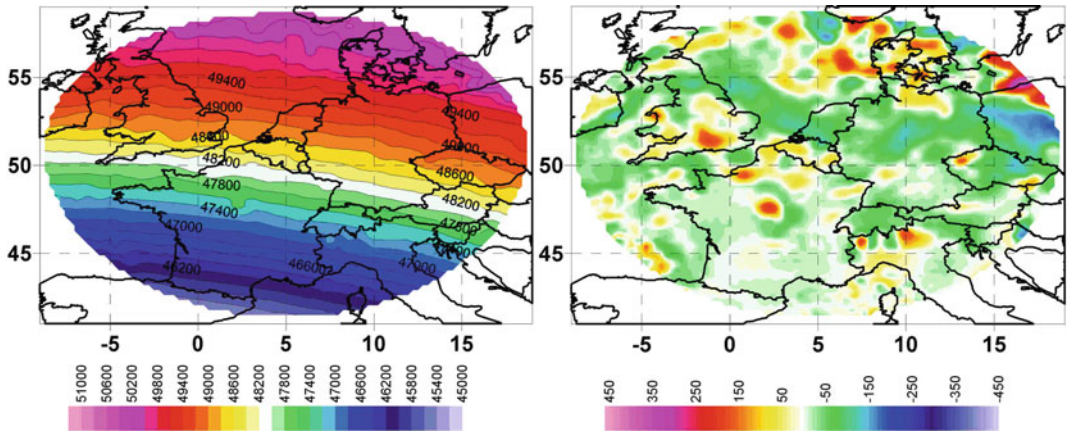

Fig. 9.1 Z component of the magnetic field at the Earth's reference radius within a Spherical Cap centred on Europe. *Left*: superimposition of the field at 2010.0 and an estimate of the crustal field (see text for details) and (*right*) the crustal field alone with about 50 km horizontal spatial resolution. Units are in nT

introduces some further level of subjectivity. Shure et al. (1982) tackled this last inconvenience by introducing the concept of harmonic splines. Concerning the localization in space, several proposals were made during the last decade, which amount to generate the Hilbert space of harmonic functions by other functions than the SH defined as β_n^m by Eq. (9.17) but still based upon Legendre polynomial expansions. Strictly speaking, these functions are only numerically localized, the counterpart being that their spectrum covers a more or less extended range of frequencies. Hereafter, we selected three representations that emerged recently in geomagnetism and we refer the reader to Shure et al. (1982) for a presentation of spherical splines (see also Langel, 1987; section 13.1).

9.3.1 Wavelets

We consider the following Dirichlet problem: to find the potential $V\left(\overrightarrow{r}\right)$, which is harmonic in the infinite shell $S(R,\infty)$ and which is known on the sphere $S(R)$. Note that R does not need to be the Earth's mean radius R_E. We assume that the potential vanishes at infinity. Thus, the Gauss coefficients g_l^m are given by the limiting expression of Eq. (9.29) when c is put to infinity

$$g_l^m = \frac{1}{4\pi R \left\| \beta_l^m \right\|^2_{L^2(S(1))}} \int_{S(1)} V(R,\theta,\varphi)\beta_l^m(\theta,\varphi)\, d\sigma, \tag{9.32}$$

where we assume that β_l^m takes real values. We adopt this formulation in order to avoid unnecessary complications with complex functions and Hermitian inner products. For the sake of convenience, we continue to select the orders m in the range $[-l,+l]$, thus adopting the notations used by other authors (Lesur, 2006; Simons and Dahlen, 2006). We further consider the β_l^m as fully normalized with respect to the inner product defined by Eq. (9.16). Following the notation of Backus et al. (1996), we define $\overrightarrow{r} = r\widehat{\mathbf{r}}$ so that Eq. (9.32) becomes

$$g_l^m = \frac{1}{4\pi R} \int_{S(1)} V(R\,\widehat{\mathbf{s}})\beta_l^m(\,\widehat{\mathbf{s}})\, d\sigma. \tag{9.33}$$

Assuming that interchanging the integration and summation makes sense, the expansion given by Eq. (9.28) may be written

$$V(r\widehat{\mathbf{r}}) = \frac{1}{4\pi R} \sum_{l=1}^{\infty} \sum_{m=-l}^{l} \int_{S(1)} \psi_l^m(r\widehat{\mathbf{r}})\beta_l^m(\widehat{\mathbf{s}})\, V(R\,\widehat{\mathbf{s}}) d\sigma, \tag{9.34}$$

$$= \frac{1}{4\pi} \int_{S(1)} V(R\widehat{\mathbf{s}}) \sum_{l=1}^{\infty} \sum_{m=-n}^{n} \left(\frac{R}{r}\right)^{l+1} \beta_l^m(\widehat{\mathbf{r}})\beta_l^m(\widehat{\mathbf{s}})\, d\sigma\,(\widehat{\mathbf{s}}), \tag{9.35}$$

where $d\sigma\,(\widehat{\mathbf{s}})$ means that the integration on the unit sphere is performed with respect to the variable $\widehat{\mathbf{s}}$. Eq. (9.35) is more concise using the spherical harmonic addition theorem (Backus et al., 1996, p. 62)

$$\sum_{m=-l}^{l} \beta_l^m(\widehat{\mathbf{r}})\beta_l^m(\widehat{\mathbf{s}}) = (2l+1)\, P_l(\widehat{\mathbf{r}}\cdot\widehat{\mathbf{s}}), \tag{9.36}$$

where P_l is the Legendre polynomial of degree l (which expression must be consistent with the norm chosen for β_l^m). We obtain finally

$$V(r\widehat{\mathbf{r}}) = \frac{1}{4\pi} \int_{S(1)} K(r\widehat{\mathbf{r}},\widehat{\mathbf{s}}) V(R\widehat{\mathbf{s}}) d\sigma\,(\widehat{\mathbf{s}}), \tag{9.37}$$

with

$$K(r\widehat{\mathbf{r}},\widehat{\mathbf{s}}) = \sum_{l=1}^{\infty} (2l+1) \left(\frac{R}{r}\right)^{l+1} P_l(\widehat{\mathbf{r}}\cdot\widehat{\mathbf{s}}). \tag{9.38}$$

Equation (9.37) teaches us that the potential V can be computed at any point $r\widehat{\mathbf{r}}$ within the infinite shell $S(R,\infty)$ by an integral transform based upon the kernel $K(r\widehat{\mathbf{r}},\widehat{\mathbf{s}})$, which maps the potential known on the boundary $S(R)$ to the potential at any point $r\widehat{\mathbf{r}}$. Note that this formalism is defined for $r > R$,where R is the chosen reference surface (again not necessarily Earth's mean radius and it could be the core mantle boundary, see Constable et al., 1993, for instance). Eq. (9.37) and (9.38) are the departure point of many representation using the global support. Constable et al., (1993; Appendix) expanded Eq. (9.38) making use of the generating Legendre polynomials and called $K(r\widehat{\mathbf{r}},\widehat{\mathbf{s}})$ the Green's function. In a recent paper presented during the IAGA in Sopron, Stockmann et al. (2009) used this kernel and a spherical triangle tesselation to estimate from satellite data the lithospheric field near the Earth's surface. In fact, Eq. (9.37) and (9.38) may be obtained when one takes the Poisson integral kernel

as a departure point (Kellog, 1929, p. 251), hence the name of Poisson wavelet generally given to this solution. Eq. (9.37) also writes

$$V(r\widehat{\mathbf{r}}) = \langle K(r\widehat{\mathbf{r}},\widehat{\mathbf{s}}), V(R\widehat{\mathbf{s}})\rangle_{L^2(S(1))}\,, \tag{9.39}$$

which is the definition of the convolution on the sphere (Holschneider et al., 2003). In addition, Eq. (9.37) looks like defining $K(r\widehat{\mathbf{r}},\widehat{\mathbf{s}})$ as being a reproducing kernel on the Hilbert space $L^2\left(S\left(R,\infty\right)\right)$, the subtlety being that the equality (9.37) has to be interpreted in terms of the norm of $L^2\left(S\left(R,\infty\right)\right)$ and not in terms of a pointwise equality between functions (see Backus et al., 1996, section 3.3 for a definition and properties of reproducing kernels). The kernel $K(r\widehat{\mathbf{r}},\widehat{\mathbf{s}})$ has another important property regarding the construction of spherical wavelets or scaling functions since it can be interpreted as the rotated function $K(r\widehat{\mathbf{e}}_z\cdot\widehat{\mathbf{s}})$ in the rotation $R_{\widehat{\mathbf{r}}}$ on the sphere such as $\widehat{\mathbf{r}} = R_{\widehat{\mathbf{r}}}\left(\widehat{\mathbf{e}}_z\right)$. Here, $\widehat{\mathbf{e}}_z$ is the unit vector carried by the axis Oz of the Cartesian reference frame to which the spherical coordinate θ is referred (see Backus et al., 1996, p.59, for further details about rotations on the sphere). Knowing that

$$K(r\widehat{\mathbf{e}}_z,\widehat{\mathbf{s}}) = \sum_{l=1}^{\infty}(2l+1)\left(\frac{R}{r}\right)^{l+1}P_l\left(\widehat{\mathbf{e}}_z\cdot\widehat{\mathbf{s}}\right), \tag{9.40}$$

Eq. (9.40) shows that $K(r\widehat{\mathbf{e}}_z,\widehat{\mathbf{s}})$, regarded as a function of $\widehat{\mathbf{s}}$, is the sum of zonal spherical harmonics in the usual sense, and, therefore, is itself a zonal function. Therefore, $K(r\widehat{\mathbf{r}},\widehat{\mathbf{s}})$ is a zonal function around the axis defined by the unit vector $\widehat{\mathbf{r}}$.

If $r = R$, the series (Eq. 9.40) no longer converges in a classical sense and cannot be used to define a wavelet transform (actually, $K(r\widehat{\mathbf{r}},\widehat{\mathbf{s}}) \to \delta\left(\widehat{\mathbf{r}},\widehat{\mathbf{s}}\right)$, the Dirac distribution when $r \to R$, see Simons et al., 2006). This inconvenience is mitigated in spherical wavelets and scaling functions theory by a flexible modification of the kernel, which then writes

$$K(r\widehat{\mathbf{e}}_z,\widehat{\mathbf{s}}) = \sum_{l=1}^{\infty}(2l+1)\,\gamma\,(l)\left(\frac{R}{r}\right)^{l+1}P_l\left(\widehat{\mathbf{e}}_z\cdot\widehat{\mathbf{s}}\right), \tag{9.41}$$

where γ is an appropriate function defined on $\mathbb{N}$ which gives sense to the infinite sum for $r = R$. Furthermore, the well-known scaling in wavelet theory is introduced through a dilation generator D_a (Holschneider, 1995, p. 3, Freeden and Michel, 2000, p. 209), which define a dilated function $\gamma\,(an)$ by

$$D_a\left(\gamma\,(n)\right) = \gamma\,(an)\,, \tag{9.42}$$

where a is a real positive number. Finally, the modified kernel writes

$$K_a(r\widehat{\mathbf{e}}_z,\widehat{\mathbf{s}}) = \sum_{l=1}^{\infty}(2l+1)\,\gamma\,(al)\left(\frac{R}{r}\right)^{l+1}P_l\left(\widehat{\mathbf{e}}_z\cdot\widehat{\mathbf{s}}\right). \tag{9.43}$$

Equation (9.43) is a relevant expression for introducing wavelets and scaling functions.

9.3.1.1 Poisson Wavelets

We focus on the family of Poisson wavelets, which are scalar wavelets that were proposed by Holschneider et al. (2003), because it has a simple and attractive interpretation in terms of multipolar potentials. The properties of the wavelets require so-called admissibility conditions on the function γ. According to the expression given in Panet et al. (2006), the Poisson wavelets write (not to be confused with g_n^m the SH Gauss coefficients)

$$g_a^n\left(r\widehat{\mathbf{r}}\right) = \frac{1}{R}\sum_{l=1}^{\infty}(2l+1)\,e^{-al}\,(al)^n\left(\frac{R}{r}\right)^{l+1}P_l\left(\widehat{\mathbf{e}}_z\cdot\widehat{\mathbf{r}}\right). \tag{9.44}$$

Between Eqs. (9.43) and (9.44), the function γ takes the particular expression $\gamma(t) = e^{-t}t^n$. We denote $g^n_{\widehat{\mathbf{s}},a}\left(r\widehat{\mathbf{r}}\right)$ the scalar field derived from $g_a^n\left(r\widehat{\mathbf{r}}\right)$ by a rotation $R_{\widehat{\mathbf{s}}}$ and write

$$g^n_{\widehat{\mathbf{s}},a}\left(r\widehat{\mathbf{r}}\right) = \frac{1}{R}\sum_{l=1}^{\infty}(2l+1)\,e^{-al}\,(al)^n\left(\frac{R}{r}\right)^{l+1}P_l\left(\widehat{\mathbf{s}}\cdot\widehat{\mathbf{r}}\right). \tag{9.45}$$

As mentioned above, the wavelet family g_a^n (Eq. 9.44) has an interesting interpretation in terms of multipoles. Consider the potential

$$\psi_n^{\lambda}(r\widehat{\mathbf{r}}) = \left[\lambda\partial_{z'}\circ\left(z'\partial_{z'}\right)\circ\ldots\circ\left(z'\partial_{z'}\right)\right]\frac{1}{|r\widehat{\mathbf{r}}-r'\widehat{\mathbf{r}}'|}, \tag{9.46}$$

where the derivatives are taken n times, $r\widehat{\mathbf{r}} = x\widehat{\mathbf{e}}_x + y\widehat{\mathbf{e}}_y + z\widehat{\mathbf{e}}_z$, $r'\widehat{\mathbf{r}}' = z'\widehat{\mathbf{e}}_z$, and λ is an arbitrary,

dimensionless constant. Developing the derivations between brackets, Eq. (9.46) becomes

$$\psi_n^\lambda(r\widehat{\mathbf{r}}) = \sum_{k=1}^{n} C_n^k \lambda^k \left(\partial_{z'}^k \frac{1}{|r\widehat{\mathbf{r}} - r'\widehat{\mathbf{r}}'|} \right)_{z'=\lambda R}, \quad (9.47)$$

where the coefficients C_n^k are computed recursively using the recurrence relation $C_k^n = C_{k-1}^{n-1} + kC_k^{n-1}, k = 1, \ldots, n-1$, with the convention $C_0^{n-1} = C_n^{n-1} = 0$. Each term $\lambda^k \left(\partial_{z'}^k \frac{1}{|r\widehat{\mathbf{r}} - r'\widehat{\mathbf{r}}'|} \right)_{z'=\lambda R}$ is a zonal multipole of order k, having k identical axes along Oz and located at the point $(0, 0, \lambda R)$. Thus, ψ_n^λ is the sum of n zonal multipoles of orders ranging from 1 (dipole) to n, all located on the Oz axis, at the point $(0, 0, \lambda R)$. It may be shown, using the expansion of $\frac{1}{|r\widehat{\mathbf{r}} - r'\widehat{\mathbf{r}}'|}$ in terms of Legendre polynomials, that

$$\psi_n^\lambda(r\widehat{\mathbf{r}}) = \frac{1}{r} \sum_{l=1}^{\infty} \lambda^l l^n \left(\frac{R}{r} \right)^l P_l \left(\widehat{\mathbf{r}} \cdot \widehat{\mathbf{e}}_z \right). \quad (9.48)$$

Writing now $\lambda = e^{-a}$, the potential ψ_n^λ takes the form

$$\psi_n^\lambda(r\widehat{\mathbf{r}}) = \frac{a^{-n}}{R} \sum_{l=1}^{\infty} e^{-al} (al)^n \left(\frac{R}{r} \right)^{l+1} P_l \left(\widehat{\mathbf{r}} \cdot \widehat{\mathbf{e}}_z \right). \quad (9.49)$$

Comparing Eq. (9.49) with Eq. (9.44), we obtain

$$g_n^a \left(r\widehat{\mathbf{r}} \right) = a^n \left(2\psi_{n+1}^\lambda(r\widehat{\mathbf{r}}) + \psi_n^\lambda(r\widehat{\mathbf{r}}) \right). \quad (9.50)$$

Thus, the wavelet $g_n^a \left(r\widehat{\mathbf{r}} \right)$ is the sum of the potentials produced by a set of $(n+1)$ zonal multipoles, with orders ranging from 1 to $(n+1)$, having all their axes along Oz, and located at $(0, 0, R\exp(-a))$. The rotational properties of $g_{\widehat{\mathbf{s}}, a}^n$ (Eq. 9.45) are such that $g_{\widehat{\mathbf{s}}, a}^n$ is the sum of the same multipoles located at point $R\exp(-a)\widehat{\mathbf{s}}$ with axes along the direction defined by the unit vector $\widehat{\mathbf{s}}$.

The set $\left\{ g_{\widehat{\mathbf{s}}, a}^n \right\}$ is a continuous family of wavelets, where $\widehat{\mathbf{s}}$ defines the radial axis $\Delta\left(\widehat{\mathbf{s}}\right)$ carrying the set of $(n+1)$ multipoles as well as the direction of the axes of the multipoles, and a refers to the location of the multipoles on Δ. In practice, the number of data being finite, the family $\left\{ g_{\widehat{\mathbf{s}}, a}^n \right\}$ must be discretized. This operation leads to the concept of a frame in the Hilbert space H of the harmonic functions belonging to $L^2\left(S\left(R, \infty\right)\right)$. A frame is a generating system which linear combinations are dense in the Hilbert space, the elements of the frame being neither linearly independent nor orthogonal to each other. Holschneider et al. (2003) provided some qualitative evidences about the completeness of the frame by comparing the dimensions of wavelet and spherical harmonic subspaces and by computing misfits between spherical harmonics and their approximation by a finite series of discrete wavelets.

Discretizing the dilation factor a (the depth of the $(n+1)$ multipoles) is straightforward but requires the definition of a reference radius R. Various spheres of geophysical importance may be used, for instance core-mantle boundary, which may offer more flexibility in the distribution of the depths of the multipoles (see Chambodut et al., 2005). The discretizing of the directions $\Delta\left(\widehat{\mathbf{s}}\right)$ is, however, a more heavy task, connected to the long standing difficulty of defining a quasi-uniform distributions of a finite number of points on the sphere (Holschneider et al., 2003; Chambodut et al., 2005).

The inverse problem formally consists in approximating a potential $V\left(r\widehat{\mathbf{r}}\right)$ with a linear combination of a given finite subspace of a frame of discrete wavelets. This writes

$$W_V(\overrightarrow{r}) = \sum_{j=1}^{J} \sum_{k=1}^{K} \alpha_{j,k} g_{\widehat{\mathbf{s}}(j), a(k)}^n \left(\overrightarrow{r} \right), \quad (9.51)$$

where the discrete family $\left\{ g_{\widehat{\mathbf{s}}(j), a(k)}^n \right\}$ has been indexed according to a pair of indexes (j, k) for the sake of clarity. Actually, for inversion purposes, a single indexing was used by Holschneider et al. (2003). W_V is the approximation of V in the subspace spanned by the wavelets $g_{\widehat{\mathbf{s}}(k), a(k)}^n$. There is a fundamental difficulty raised by the redundancy of the wavelet frame. Whereas the Gauss coefficients are theoretically unique, the coefficients α_k are not. Therefore, the inverse problem is by essence ill-conditioned and requires some regularization. Fortunately, the wavelets have convenient properties with respect to the inner product on $L^2\left(S\left(1\right)\right)$ that allows the quadratic term involved in the smoothness constraint to be written in a concise form. The reader is referred to Holschneider et al. (2003), Chambodut et al. (2005) and Panet et al. (2006) for applications in geomagnetism and geodesy.

9.3.1.2 Multi-scale Modelling

Mayer and Maier (2006) proposed a modelling of CHAMP satellite measurements based upon vector scaling functions as an alternative to the Mie representation. However, we discuss the expression for the scalar potential only that was elaborated by Maier (2003, Chapter 4), and was applied to the crustal field modelling by Maier and Mayer (2003). More specifically, they proposed a multi-scale method for downward continuation of the crustal field estimated at satellite altitude. A less sophisticated and older approach based on scalar data may also be found in Achache et al. (1987). The method may apply to vector data but hereafter we restrict ourselves to the radial component modelling. The problem is the following: how from the given radial component B_r known over the surface of a sphere of radius r can we express B_r over a lower spherical surface R. The solution in terms of spherical harmonics is of course well-known (for instance Maus et al. 2007a), but we review it because, first, it is interesting to see which advantages could be drawn from the flexibility of the wavelet representation, second, it is the heart of many problems in geomagnetism, and thus regional modelling. We start again with the expansion (9.28) and we assume internal fields only. The radial component then simply writes

$$B_r\left(r\widehat{\mathbf{r}}\right) = -\partial_r V = \sum_{l=1}^{\infty}\sum_{m=-l}^{l} g_l^m\left(l+1\right)\left(\frac{R}{r}\right)^{l+2}\beta_l^m\left(\widehat{\mathbf{r}}\right). \tag{9.52}$$

As in the previous section, β_l^m is a real, normalized, spherical harmonic function and $r \geq R$. We remark that rB_r is itself an harmonic function in $S\left(R,\infty\right)$. In particular for $r = R$

$$RB_R\left(R\widehat{\mathbf{r}}\right) = R\sum_{l=1}^{\infty}\sum_{m=-l}^{l} g_l^m\left(l+1\right)\beta_l^m\left(\widehat{\mathbf{r}}\right). \tag{9.53}$$

where B_R stands for B_r calculated on the sphere $S\left(R\right)$. The coefficients $Rg_l^m\left(l+1\right)$ are obtained straightforwardly by

$$Rg_l^m\left(l+1\right) = \frac{1}{4\pi}\int_{S(1)} \beta_l^m\left(\widehat{\mathbf{r}}\right) RB_R\left(R\widehat{\mathbf{r}}\right) d\sigma. \tag{9.54}$$

Introducing the expression of $g_l^m\left(l+1\right)$ into Eq. (9.52), we obtain a relationship between $rB_r\left(r\widehat{\mathbf{r}}\right)$ and $RB_R\left(R\widehat{\mathbf{s}}\right)$ similar to that given by Eq. (9.37)

$$rB_r\left(r\widehat{\mathbf{r}}\right) = \frac{1}{4\pi}\int_{S(1)} K\left(r\widehat{\mathbf{r}},\widehat{\mathbf{s}}\right) RB_R\left(R\widehat{\mathbf{s}}\right) d\sigma\left(\widehat{\mathbf{s}}\right), \tag{9.55}$$

with $K\left(r\widehat{\mathbf{r}},\widehat{\mathbf{s}}\right)$ being explicitly written in Eq. (9.38). $K\left(r\widehat{\mathbf{r}},\widehat{\mathbf{s}}\right)$ is the kernel of an operator designated by Λ_{AP}, according to Maier (2003, p. 99), which links rB_r to RB_R. Formally

$$\Lambda_{AP}\left(RB_R\right) = rB_r. \tag{9.56}$$

RB_R (respectively rB_r) is an element of the Hilbert space $L^2\left(S\left(R\right)\right)$ (respectively $L^2\left(S\left(r\right)\right)$), the inner product on $L^2\left(S\left(\rho\right)\right)$ ($\rho = R$ or r) being defined by Eq. (9.16). With respect to this inner product, the functions

$$Y_{\rho,l}^m\left(\rho\widehat{\mathbf{r}}\right) = \beta_l^m\left(\widehat{\mathbf{r}}\right), \tag{9.57}$$

are still orthonormal (note that we use explicit notations to designate elements belonging to each of the spaces $L^2\left(S\left(R\right)\right)$ and $L^2\left(S\left(r\right)\right)$). Λ_{AP} is an operator mapping the Hilbert space $L^2\left(S\left(R\right)\right)$ onto the Hilbert space $L^2\left(S\left(r\right)\right)$ and defines the upward continuation operation. It may be shown that its adjoint operator Λ_{AP}^* is given by

$$\Lambda_{AP}^* rB_r\left(r\widehat{\mathbf{r}}\right) = \frac{1}{4\pi}\int_{S(1)} K\left(r\widehat{\mathbf{r}},\widehat{\mathbf{s}}\right) rB_r\left(r\widehat{\mathbf{s}}\right) d\sigma\left(\widehat{\mathbf{s}}\right), \tag{9.58}$$

and that $\psi_{R,l}^m$ (respectively $\psi_{r,l}^m$) is an eigenvector of Λ_{AP} (respectively Λ_{AP}^*) associated to the eigenvalue

$$\sigma_l = \left(\frac{R}{r}\right)^{l+1}. \tag{9.59}$$

Thus, the limit of σ_l, when l tends toward infinity, is 0 and there is no theoretical difficulty in the calculation of rB_r knowing RB_R (Eq. 9.56). In general, we also face the problem of calculating RB_R knowing rB_r because small scales are geometrically more enhanced than larger scales with downward continuation. The

difficulty is more explicit if we write rB_r in terms of spherical harmonics

$$rB_r = \sum_{l=1}^{\infty} \sum_{m=-l}^{l} q_l^m Y_{r,l}^m \quad \text{with} \quad q_l^m = \left\langle rB_r, Y_{r,l}^m \right\rangle_{L^2(S(r))}. \tag{9.60}$$

Using Eqs. (9.56, 9.60) and the above-mentioned properties of $Y_{R,l}^m$ and $Y_{r,l}^m$ with respect to the operators Λ_{AP} and Λ_{AP}^* respectively, we obtain

$$\Lambda_{AP}^* \circ \Lambda_{AP}\left(RB_R\right) = \sum_{l=1}^{\infty} \sum_{m=-l}^{l} \sigma_l q_l^m Y_{R,l}^m. \tag{9.61}$$

On the other hand, we are looking for the expansion of RB_R of the form

$$RB_R = \sum_{l=1}^{\infty} \sum_{m=-l}^{l} p_l^m Y_{R,l}^m. \tag{9.62}$$

Applying the operator $\Lambda_{AP}^* \circ \Lambda_{AP}$ to this expansion, we obtain

$$\Lambda_{AP}^* \circ \Lambda_{AP}\left(RB_R\right) = \sum_{l=1}^{\infty} \sum_{m=-l}^{l} \sigma_l^2 p_l^m Y_{R,l}^m. \tag{9.63}$$

Comparing it to expression (9.61) and using $\Lambda_{AP}\left(Y_{R,l}^m\right) = \sigma_l Y_{R,l}^m$, we obtain finally

$$RB_R = \sum_{l=1}^{\infty} \sum_{m=-l}^{l} \sigma_l^{-1} \left\langle rB_r, Y_{r,l}^m \right\rangle_{L^2(S(r))} Y_{R,l}^m. \tag{9.64}$$

Equation (9.64) makes the generalized, Moore-Penrose, inverse of Λ_{AP} explicit. Hereafter, we denote Λ_{AP}^+ this generalized inverse (hence, formally, $RB_R = \Lambda_{AP}^+\left(rB_r\right)$). Due to the behavior of σ_l^{-1}, the convergence of the double series is by no means ensured and some regularization method has to be invoked. It is precisely at this point that the multi-scaling approach can be involved. We assume for a while that Eq. (9.64) makes sense, and we split this expression into two successive operations following Freeden et al. (1999)

$$A^D\left(R\widehat{\mathbf{r}}\right) = \sum_{l=1}^{\infty} \sum_{m=-l}^{l} \sigma_l^{-1/2} \left\langle rB_r, Y_{r,l}^m \right\rangle_{L^2(S(r))} Y_{r,l}^m\left(\widehat{\mathbf{r}}\right), \tag{9.65}$$

and

$$A^R\left(R\widehat{\mathbf{r}}\right) = \sum_{l=1}^{\infty} \sum_{m=-l}^{l} \sigma_l^{-1/2} \left\langle A^D, Y_{R,l}^m \right\rangle_{L^2(S(R))} Y_{R,l}^m\left(\widehat{\mathbf{r}}\right). \tag{9.66}$$

It may be shown that $A^R\left(R\widehat{\mathbf{r}}\right) = RB_R\left(R\widehat{\mathbf{r}}\right)$, at least formally. Now, Eq. (9.65) may be written as a mapping from $L^2\left(S\left(r\right)\right)$ onto $L^2\left(S\left(R\right)\right)$, which gives $A^D\left(R\widehat{\mathbf{r}}\right)$ knowing $rB_r\left(r\widehat{\mathbf{s}}\right)$. Likewise, Eq. (9.66) is an internal mapping on $L^2\left(S\left(R\right)\right)$. Each of these mappings is expressed through an integral equation using a kernel Φ

$$A^D\left(R\widehat{\mathbf{r}}\right) = \frac{1}{4\pi} \int_{S(1)} \Phi^D\left(\widehat{\mathbf{r}}, \widehat{\mathbf{s}}\right) rB_r\left(r\widehat{\mathbf{s}}\right) d\sigma\left(\widehat{\mathbf{s}}\right), \tag{9.67}$$

with

$$\begin{aligned} \Phi^D\left(\widehat{\mathbf{r}}, \widehat{\mathbf{s}}\right) &= \sum_{l=1}^{\infty} \sum_{m=-l}^{l} \sigma_l^{-1/2} Y_{R,l}^m\left(\widehat{\mathbf{r}}\right) Y_{r,l}^m\left(\widehat{\mathbf{s}}\right) \\ &= \sum_{l=1}^{\infty} \sigma_l^{-1/2} \left(2l+1\right) P_l\left(\widehat{\mathbf{r}} \cdot \widehat{\mathbf{s}}\right), \end{aligned} \tag{9.68}$$

and

$$A^R\left(R\widehat{\mathbf{r}}\right) = RB_R\left(R\widehat{\mathbf{r}}\right) = \frac{1}{4\pi} \int_{S(1)} \Phi^R\left(\widehat{\mathbf{r}}, \widehat{\mathbf{s}}\right) A^D\left(R\widehat{\mathbf{s}}\right) d\sigma\left(\widehat{\mathbf{s}}\right), \tag{9.69}$$

with

$$\begin{aligned} \Phi^R\left(\widehat{\mathbf{r}}, \widehat{\mathbf{s}}\right) &= \sum_{l=1}^{\infty} \sum_{m=-l}^{l} \sigma_l^{-1/2} Y_{R,l}^m\left(\widehat{\mathbf{r}}\right) Y_{R,l}^m\left(\widehat{\mathbf{s}}\right) \\ &= \sum_{l=1}^{\infty} \sigma_l^{-1/2} \left(2l+1\right) P_l\left(\widehat{\mathbf{r}} \cdot \widehat{\mathbf{s}}\right). \end{aligned} \tag{9.70}$$

On the right-hand sides of Eqs. (9.68) and (9.70), we have applied the addition theorem (Eq. 9.36) and we recognize, again, the expressions in terms of Legendre polynomials. Of course, $\Phi = \Phi^D = \Phi^R$ but their expressions are formally different for the sake of clarity, Φ^D being the kernel of an operator mapping $L^2\left(S\left(r\right)\right)$ onto $L^2\left(S\left(R\right)\right)$ and Φ^R being the kernel of an operator on $L^2\left(S\left(R\right)\right)$. The right-hand sides of Eqs. (9.68) and (9.70) show that the series do not converge. In order to remedy this drawback,

Freeden et al. (1999) replaced the problematic coefficients $\sigma_l^{-1/2}$ by a family of coefficients $\{\gamma_j(l)\}$ called filters, j, being a positive or negative integer. The kernel $\Phi_j^D(\widehat{\mathbf{r}},\widehat{\mathbf{s}})$, for which $\sigma_l^{-1/2}$ is replaced by $\gamma_j(l)$, is called regularization decomposition kernel whereas $\Phi_j^R(\widehat{\mathbf{r}},\widehat{\mathbf{s}})$ is called regularization reconstruction kernel. We define $A_j^D(R\widehat{\mathbf{r}})$ and $A_j^R(R\widehat{\mathbf{r}})$ the functions obtained in Eqs. (9.65) and (9.66), with $\sigma_l^{-1/2}$ replaced by $\gamma_j(l)$. These functions are smoothed, and approximate, versions of the exact solutions A^D and A^R. If the families $\{\gamma_j(l)\}$ verify appropriate constraints (see Freeden et al., 1999, for the details and for some relevant functions $l \to \gamma_j(l)$) it may be shown that $\lim_{j\to\infty} \left\| A_j^R(R\widehat{\mathbf{r}}) - \Lambda_{AP}^+(rB_r) \right\|_{L^2(S(R))} = 0$, which is obviously a desired property of the regularization. The regularized solution finally writes

$$A_j^R(R\widehat{\mathbf{r}}) = P_j(rB_r) = \frac{1}{16\pi^2} \int_{S(1)} \int_{S(1)} \Phi_j^R(\widehat{\mathbf{r}},\widehat{\mathbf{s}})\, \Phi_j^D(\widehat{\mathbf{s}},\widehat{\mathbf{t}})\, rB_r(r\widehat{\mathbf{t}})\, d\sigma(\widehat{\mathbf{t}})\, d\sigma(\widehat{\mathbf{s}}). \tag{9.71}$$

P_j being defined by the right-hand side and being an approximation of $\bigwedge_{AP}^+$. The functions rB_r that are upward continuations onto the sphere $S(r)$ of radial components known on the sphere $S(R)$, belong to the range $Image(\Lambda_{AP}) \subset L^2(S(r))$ of Λ_{AP}. This implies that $A_j^R = P_j(rB_r)$ belongs to the subspace $V_j = \{P_j(f) \mid f \in Image(\Lambda_{AP})\}$. It may be shown that $V_j \subset V_{j'}$ when $j < j'$ and that the closure of $\lim_{j\to\infty} V_j = L^2(S(R))$. Thus the solution of the generalized inverse problem may be approximated to arbitrary accuracy (in the sense of $\|\cdot\|_{L^2(S(R))}$) by increasing the scaling index j. However, every approximation $A_j^R(R\widehat{\mathbf{r}})$ has to be computed by means of a numerical surface integration. Freeden et al. (1999) suggest a possibly more efficient way. The decomposition $\Psi_j^D(\widehat{\mathbf{r}},\widehat{\mathbf{s}})$ and reconstruction $\Psi_j^R(\widehat{\mathbf{r}},\widehat{\mathbf{s}})$ wavelets take the same expressions as the corresponding decomposition and reconstruction kernels when the family of coefficients $\{\gamma_j(l)\}$ is replaced by the family $\{\varphi_j(l)\}$

$$\varphi_j(l) = \left[(\gamma_{j+1}(l))^2 - (\gamma_j(l))^2 \right]^{1/2}. \tag{9.72}$$

Using $\Psi_j^D(\widehat{\mathbf{r}},\widehat{\mathbf{s}})$ and $\Psi_j^R(\widehat{\mathbf{r}},\widehat{\mathbf{s}})$, Freeden et al. (1999) define a new operator R_j

$$R_j(rB_r) = \frac{1}{16\pi^2} \int_{S(1)} \int_{S(1)} \Psi_j^R(\widehat{\mathbf{r}},\widehat{\mathbf{s}})\, \Psi_j^D(\widehat{\mathbf{s}},\widehat{\mathbf{t}})\, rB_r(r\widehat{\mathbf{t}})\, d\sigma(\widehat{\mathbf{t}})\, d\sigma(\widehat{\mathbf{s}}), \tag{9.73}$$

and subspaces $W_j = \{R_j(f) \mid f \in Image(\Lambda_{AP})\}$. It may be shown that $P_J(rB_r) = P_0(rB_r) + \sum_{j=0}^{J-1} R_j(rB_r)$ and that $V_J = V_0 \oplus \sum_{j=0}^{J} W_j$ where the symbol $\oplus$ stands for the direct sum of the subspaces W_j. Thus, V_0 and $\{W_j\}_{j=0,\cdots J}$ are a partition of the approximation subspace V_J. Using this wavelet approach, the approximation gained at step $j+1$ is directly obtained by upgrading it from step j thanks to Eq. (9.73). However, as noticed by Maier (2003) there are some practical difficulties in the implementation. First, this method assumes data located on the sphere $S(r)$, thus neglecting altitude variations. Second, if the crustal field modelling is the target, an appropriate low-frequency global model has to be subtracted from the selected (and already processed) data. Third, since surface integrations have to be performed (Eq. 9.71 and 9.73), it is necessary to resample scattered data onto the nodal points of an appropriate grid and use integration algorithms (see Lesur and Gubbins, 1999, for a review). The multi-scale resolution was applied by Maier (2003, Chapter 4) on two spherical caps, one enclosing the Bangui anomaly and one enclosing the European continent. Due to the limited areas, Gibbs effects appeared on the boundaries that could be hidden using caps larger than the integration domain, themselves larger than the visualization caps. As we shall see in Section (9.4), this is reminiscent of a numerical 'trick' often employed in regional modelling that help artificially improving the convergence of the numerical solution by in fact implicitly imposing homogeneous conditions near the boundaries. The field is free to take any value and shape in regions with no data. This will, in turn, improve the fit in regions where data are available.

9.3.2 Localized Harmonic Functions

The localized functions proposed by Lesur (2006) are similar to the discretized Poisson wavelets described in Section (9.3.1.1) in the sense that they are linear

combinations of zonal solid spherical harmonics. However, they do not conform to the wavelet concept (described so far) because they are not constructed using a dilated mother wavelet and are band-limited. From this last viewpoint, the localized functions are closer to the Slepian functions (Section 9.4.5). The unit vectors $\widehat{\mathbf{s}}_k$ which defines the symmetry axis of the zonal spherical harmonics $P_l\left(\widehat{\mathbf{s}}_k \cdot \widehat{\mathbf{r}}\right)$ are distributed on a grid according to the following scheme

$$\begin{aligned} \theta_i &= \arccos\left(u_i\right) \;\; i = 1, \ldots, (L+1)\,; \\ \varphi_j &= \frac{2\pi j}{2L+1}\, j = 1, \ldots, (2L+1)\,, \end{aligned} \tag{9.74}$$

where u_i is the ith zero of the Legendre polynomial P_{L+1}. This distribution addresses the issue of computing spherical integrals using quadrature methods. The grid defined by Eq. (9.74) is often referred to as a Gauss-Neumann grid (see Sneeuw, 1994 and references therein). Accordingly, hereafter, we will use the double index (i, j) instead of the single one k, although it would not be difficult to map the pair (i, j) to a single index. The Gauss coefficients of an expansion $V\left(R\widehat{\mathbf{r}}\right) = R\sum_{l=1}^{L}\sum_{m=-l}^{l} g_l^m \beta_l^m\left(\widehat{\mathbf{r}}\right)$, assuming that the β_l^m are real and Schmidt quasi-normalized, are given by the classical integral

$$g_l^m = \frac{2l+1}{4\pi R}\int_{S(1)} V\left(\widehat{\mathbf{r}}\right)\beta_l^m\left(\widehat{\mathbf{r}}\right) d\sigma\,. \tag{9.75}$$

Using the grid with the associated weight

$$w_i^{L+1} = \frac{2}{1-u_i^2}\,\partial_u\left(P_{L+1}\left(u_i\right)\right)^{-2} \quad i = 1, \ldots, (L+1)\,, \tag{9.76}$$

the integral may be approximated to high accuracy, by the finite sum (Lesur, 2006)

$$g_l^m = \frac{2l+1}{2\left(2L+1\right)R}\sum_{i=1}^{L+1} w_i^{L+1}\sum_{j=1}^{2L+1} V\left(R\widehat{\mathbf{r}}_{ij}\right)\beta_l^m\left(\widehat{\mathbf{r}}_{ij}\right). \tag{9.77}$$

Now, the localized functions write

$$F_{ij}^L\left(r\widehat{\mathbf{r}}\right) = R\sum_{l=1}^{L}\sum_{m=-l}^{l}\left(\frac{R}{r}\right)^{l+1} f_l\beta_l^m\left(\widehat{\mathbf{s}}_{ij}\right)\beta_l^m\left(\widehat{\mathbf{r}}\right). \tag{9.78}$$

where the coefficient f_l is a tuning factor allowing to tighten more or less the functions $f_l\beta_l^m\left(\widehat{\mathbf{s}}_{ij}\right)\beta_l^m\left(\widehat{\mathbf{r}}\right)$ around the point $\widehat{\mathbf{s}}_{ij}$. Note that as before the functions $F_{ij}^L\left(r\widehat{\mathbf{r}}\right)$ could be again expressed in terms of Legendre polynomials $\left(\frac{R}{r}\right)^{l+1} P_l\left(\widehat{\mathbf{s}}\cdot\widehat{\mathbf{r}}\right)$ using the addition theorem. It may be shown that, like the basis functions $\left(\frac{R}{r}\right)^{l+1}\beta_l^m$, they span the space H_L of the harmonic functions in the domain $S(R,\infty)$, of maximum degree L. The dimension of H_L being $L\left(L+2\right)$, they are not linearly independent (this property is similar to the concept of frame in Section 9.3.1.1) and they do not necessarily form a basis. Thus, the coefficients γ_{ij} of the expansion

$$V\left(r\widehat{\mathbf{r}}\right) = \sum_{i=1}^{L+1}\sum_{j=1}^{2L+1}\gamma_{ij}F_{ij}^L\left(r\widehat{\mathbf{r}}\right) \tag{9.79}$$

are not unique. However, thanks to the orthogonality properties of the spherical harmonics β_l^m with respect to the quadrature expressed by Eq. (9.77), Lesur (2006) gave an elegant expression of the γ_{ij} in terms of the Gauss coefficients. In the framework of the inverse problem, Lesur (2006) discussed the choice of f_l in connection with the weight functions $w_L\left(\theta\right)$ and with the decrease rate of the gradient away from $\widehat{\mathbf{s}}_{ij}$. The inverse problem amounts to find the coefficients γ_{ij} which parameterize the model

$$\overrightarrow{B} = -\overrightarrow{\nabla}\left\{\sum_{i=1}^{L+1}\sum_{j=1}^{2L+1}\gamma_{ij}F_{ij}^L\left(r\widehat{\mathbf{r}}\right)\right\}. \tag{9.80}$$

Due to the non-uniqueness of this expansion, a smoothness constraint built *via* a damping matrix may be introduced. Localized harmonic functions are used in Lesur and Maus (2006) model globally the lithospheric field with reduced spatial resolution at high latitudes. According to Lesur and Maus (2006), this flexibility allowed reducing the spurious effects visible in the polar regions with model MF4 (Maus et al., 2006) and dealing with multi-level data.

Figure 9.2 shows a reconstruction of the crustal part of the synthetic Z_{all} data (see Fig. 9.1-right) using Eq. (9.80) with Eq. (9.78) up to $L = 400$ (about 100-km wavelength). We recall that the synthetic data are calculated to SH 720 ($L = 720$). This difference introduce some spatial aliasing in the modelling that may explain part of the observed tiny wiggles both in the

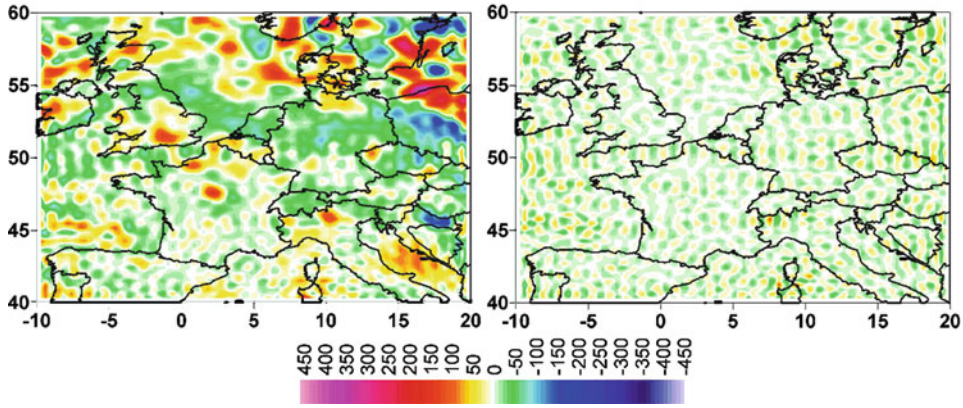

Fig. 9.2 Example of radial magnetic field reconstruction using the philosophy of band-limited functions (*left*) and the residuals (*right*) between this approximation and the original data shown in Fig. 9.1

model and the residual maps. However, the setting of the tuning factor f_l plays also a key role in the apparent stability of the modelling. Increasing the expansion of the series (9.78) and selecting a more appropriate f_l factor, for instance, would provide an almost perfect residual mean squares fit.

9.4 Modelling the Field Regionally

SH basis functions are neither well suited for modelling unevenly distributed data nor for crustal field modelling because their sensitivity at the global scale is in poor agreement with the local nature of the geological sources. We saw that only combinations of band limited and weighted SH harmonics could help circumventing this difficulty. Another philosophy, however, is to perform data fitting at a regional scale using functions with local support. Such an approach has a long history (e.g., Howarth, 2001) and we focus here on regional modelling methods based upon the resolution of the Laplace equation in a bounded domain Ω leading to Fourier-like expansions. Before proceeding further, it is important to keep in mind that the concept of internal and external field at regional scale is complicated by the existence of a lateral boundary, be it a square or a circle (or any other type of boundary). We thus assert without formally demonstrating it (but we will give some arguments below in Section 9.4.2.2) that regional basis functions are not able to distinguish between magnetic fields generated below or above the Earth's surface. Thus, if one wants to study and interpret the modelled magnetic field source, specific data pre-processing are required in order to remove unwanted contributions. We do not take much risk by further asserting that this difficulty arises also with global modelling techniques as long as they are used over a small portion of the Earth only, even though they are based on functions with global support. For this reason it is advisable to filter out the undesired magnetic field contributions, generally of external origin, before performing the regional modelling. At present, no comprehensive modelling of the magnetic field was undertaken. Some recent general reviews regarding other methods of local modelling, the availability of magnetic data at the regional scale, and applications may be found in several papers or books (Langel and Hinze, 1998; Mandea and Purucker, 2005; Purucker and Whaler, 2007 and Thébault et al. 2010, for instance).

9.4.1 Review of Modelling in the Flat Earth Approximation

Every method leading to a Fourier series expansion could be presented in a way similar to the SH formalism that is, via the resolution of a boundary value problem for the Laplace equation in the domain Ω using the method of variable separation. For some reason, this way of doing has not been systematically applied to the flat earth approximation methods as is outlined below. In these methods, the earth is locally approximated by its tangent plane and the domain of interest is built upon this plane (see Langel and

Hinze, 1998, p. 134 for a qualitative discussion about the validity of this approximation). The main advantage of this assumption is that the involved functions are much simpler to compute than in the spherical geometry.

9.4.1.1 Rectangular Harmonic Analysis

Rectangular harmonic analysis (RHA) refers to a local domain consisting in a rectangular box. Alldredge (1981, 1982, 1983) applied RHA to surface data whereas Nakagawa and Yukutake (1985) and Nakagawa et al. (1985) extended its use to the analysis of satellite data but at the expense of using an *ad-hoc* weighting to minimize edge effects. Haines (1990) made a thorough analysis on RHA which led him to suggest basis functions provided by various boundary value problems.

Let us start however with the most frequently used expansion, written in terms of periodic functions. Following the notations of Langel and Hinze (1998, p. 132), the expression of the expansion S_V of a potential V can be conveniently expressed in complex form

$$S_V(x,y,z) = X_0 x + Y_0 y + Z_0 z + \sum_{k=-K}^{K} \sum_{l=-L}^{L} \chi_{kl} \exp \left[-2\pi i \left(\frac{kx}{L_X} + \frac{ly}{L_Y} \right) \right] \exp\left(D_{kl} z\right), \tag{9.81}$$

with

$$D_{kl} = 2\pi \left(\frac{k^2}{L_X^2} + \frac{l^2}{L_Y^2} \right)^{1/2}, \tag{9.82}$$

which, apart from the linear term, is valid in the unbounded domain $]0, L_X[\times]0, L_Y[\times]0, \infty[$ with the z axis oriented positively downwards (Fig. 9.3). The potential is essentially a L_X, L_Y periodic function in an horizontal plane, and vanishes when z tends towards minus infinity. The expansion is complemented with linear terms which are intended to reduce boundary effects (Note that Eq. 9.82 has been corrected for the error in Eq. 9.5) of Alldredge, 1981, as was underlined by Malin et al., 1996)**.** Nakagawa and Yukutake (1985) and Nakagawa et al. (1985) worked on an area with square section ($L_X = L_Y$) and isotropic expansions ($K = L = 3$) whereas Alldredge used a domain with a rectangular section but restricted the sums in (9.81) by the relationship $k + l = N_{\max} + 1$. As the function to be modelled is not periodic at all, Gibbs effects are to be expected. They are all the more serious as the values at opposite boundaries are different. The linear terms, which are obviously harmonic, are intended to minimize the ringing effects and some authors (e.g., Nakagawa et al., 1985) further weighted the data in an area along the edges with a cosine taper function or even added some more terms solving Laplace equation (Malin et al., 1996).

Haines (1990) made a thorough analysis of RHA. To our knowledge, he was the first to spot the fundamental drawbacks of the original RHA expansion, the one based on periodic basis functions. Noting that these functions solve a particular boundary value problem, he suggested applying other boundary conditions that would be consistent with the properties of the function to be modelled. Haines focused his discussion on the uniform convergence properties of generalized Fourier expansions S_V. In the most general case of a regular Sturm-Liouville problem, the expansions are the solutions of the ordinary second-order differential equation on the interval $]a, b[$

$$-d_x\left(p(x) d_x f\right) + \left(q(x) - \lambda g(x)\right) = 0, \tag{9.83}$$

subject to the general mixed boundary conditions

$$\alpha_1 f(a) - \beta_1 \left(d_x f\right)_a = 0, \tag{9.84a}$$

$$\alpha_2 f(b) + \beta_2 \left(d_x f\right)_b = 0, \tag{9.84b}$$

where $p(x)$ is positive, continuously differentiable on $[a, b]$, $g(x)$ is positive and continuous, $q(x)$ is continuous. Note that $-\left(d_x f\right)_a$ and $\left(d_x f\right)_b$ are one-dimensional expressions of the normal derivative to the boundary of the domain. Setting $p(x) = g(x) = 1$ and $q(x) = 0$, and periodic boundary conditions on $f(x)$ and its derivative, we obtain the familiar expansion given by Eq. (9.81). The Dirichlet boundary value problem is defined by setting $\beta_1 = \beta_2 = 0$, whereas $\alpha_1 = \alpha_2 = 0$, define a boundary value problem of Neumann type. Note that the boundary value problem is incomplete as no condition is set neither on the lower nor the upper surface so that the solution with altitude is not a basis and thus does not necessarily agree with the

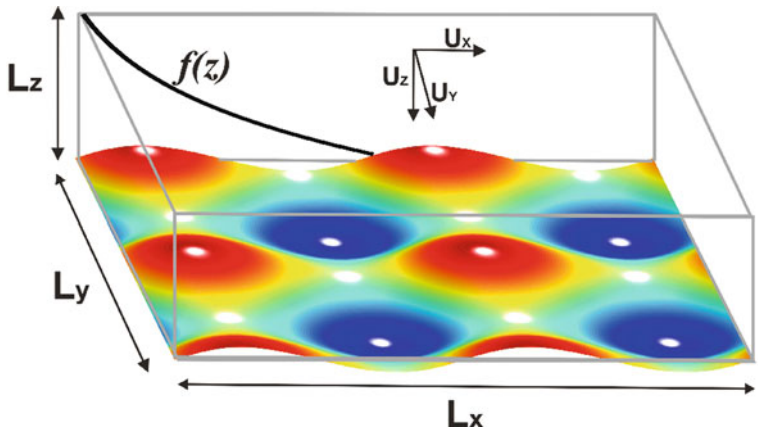

Fig. 9.3 Schematic representation of the domain of validity of the Rectangular Harmonic Analysis (RHA). The colour surface represents the rectangular harmonics for l = 3 and k = 3 (see Eq. 9.81). f(z) is the exponential radial field dependence with altitude

behavior of Newtonian potential fields with altitude. The discussions made by Haines (1990) concerning the choice of the most appropriate lateral boundary conditions rely on the Sturm-Liouville theorem (Gonzalez-Velasco, 1995, Section 4.4), which simplest expression is "*if f is continuous and satisfies the boundary conditions in Eqs. (9.84a), (9.84b) and f′ piecewise continuous on* $[a, b]$*, the generalized Fourier series* S_f *converges absolutely and uniformly towards f on* $[a, b]$".

In the absence of magnetic sources close to the boundary of the domain, the regularity conditions are fulfilled by the magnetic potential under consideration. However, the magnetic potential in general verifies neither Neumann nor Dirichlet nor mixed boundary conditions, which is particularly troublesome. In this case, the problem is no longer self-adjoint (i.e., the basis is not orthonormal) and becomes by far more difficult (Coddington, 1955, Chapter 12). The simplest way to overcome the difficulty, as advocated by Haines (1990), is to mix up basis functions of self-adjoint problems. This solution should preserve uniform convergence but at the expense of introducing non-orthogonal basis functions. Another way of circumventing the difficulty is to deal with potentials having wavelengths shorter than the dimension of the domain, thus reduced values on the boundary, closer to Dirichlet or Neumann conditions. These arguments should be kept in mind as they are particularly important to understand some of the properties of Spherical Cap Harmonic Analysis discussed in Section (9.4.2.2).

Figure 9.4 illustrates this previous discussion. The model is obtained by inverting the synthetic data Z_{all} (see Section 9.2.3) with the basis functions defined by $Z = -\partial_z S_V(x, y, z)$ using Eq. (9.81); thus without setting specific boundary conditions. The maximum series expansion defines a minimum wavelengths of about 100 km. As can be verified, the RHA does quite well in modelling single surface data and is able to represent both large (core) and small (crustal) wavelengths up to the required resolution. However, the residual map exhibits long oscillation, spreading from the edges to the center of the rectangle, that is symptomatic of Gibbs effect. The slight curvature in these large residuals also show the consequence of the flat Earth approximation. Whether or not the shape and magnitude of residuals are significant is a matter of judgement left to the reader as, in practice, it depends on the purpose for which the model is derived. The non-orthogonality of the basis functions is another property that forbids us to carry out spectral analyses and restricts ourselves to relatively low series expansion since expanding the series further keeps degrading the conditioning of the inverse matrix. Note that such a spectrum would anyway be difficult to interpret because of spatial aliasing unless some detrending is carried out *prior* to the inversion. At last, introducing data measured at different altitudes does not provide satisfactory solutions because the radial functions are

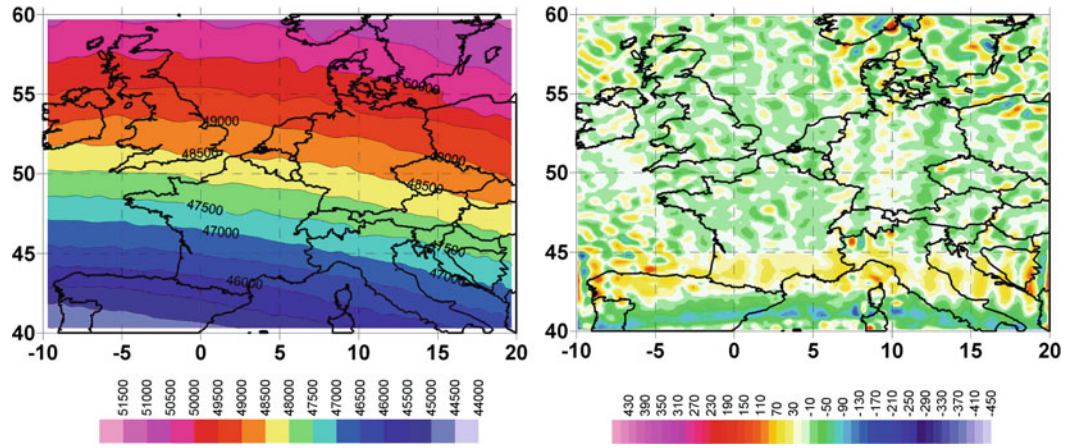

Fig. 9.4 Example of Rectangular Harmonic Analysis using the Z vector component only. The obtained RHA model (*left*) and the residuals between the model and data (*right*) illustrate some of the properties discussed in the text. Units are in nT

not designed for it. Setting appropriate boundary conditions on each surface of the whole domain (including upper and lower surfaces) would likely alleviate part of these practical difficulties.

9.4.1.2 Cylindrical Harmonic Analysis

Alldredge (1982) also studied the solutions of the Laplace equation in a circular cylindrical region. The vertical axis of the area is its axis of symmetry and its lateral boundary a cylinder of radius ρ (Fig. 9.5). In cylindrical coordinates (r, θ, z), the Laplace equation writes

$$\frac{1}{r}\partial_r\left(r\partial_r V\right) + \frac{1}{r^2}\partial^2_{\theta^2} V + \partial^2_{z^2} V = 0. \tag{9.85}$$

The method of variable separation, with $V(r, \theta, z) = R(r)T(\theta)Z(z)$ leads to the following set of ordinary differential equations

$$d^2_{z^2} Z = \mu^2 Z, \tag{9.86a}$$

$$r^2 d^2_{r^2} R + r d_r R + \left(\mu^2 r^2 - \lambda^2\right) R = 0, \tag{9.86b}$$

$$d^2_{\theta^2} T = -\lambda^2 T, \tag{9.86c}$$

where μ^2 and λ^2 are *a priori* complex constants. Equation (9.86c) associated to 2π-periodic conditions for the function and its first derivative, leads to the condition $\lambda = m$, positive integer and to the familiar solution

$$T(\theta) = A_m \mathrm{e}^{im\theta} + B_m \mathrm{e}^{-im\theta}. \tag{9.87}$$

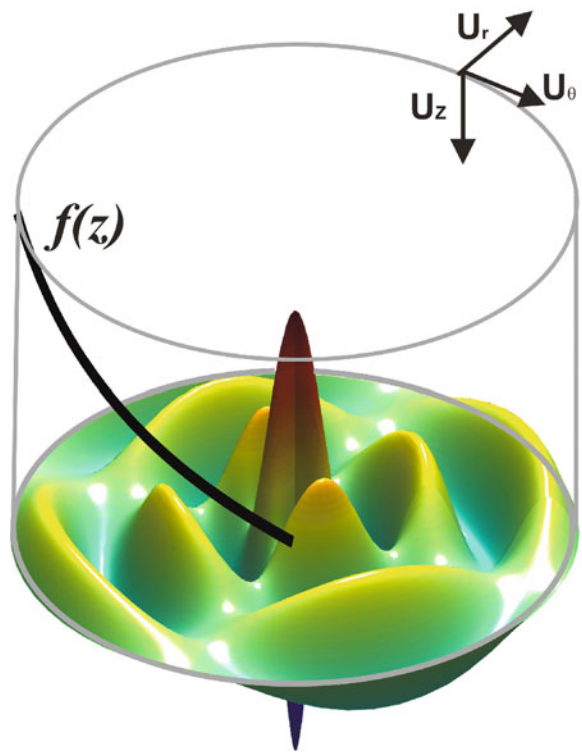

Fig. 9.5 Schematic representation of the domain of validity of the Cylindrical Harmonic Analysis (CHA). The colour surface represents the cylindrical harmonics for $m = 2$ and $k = 2$ (see Eq. 9.92). f(z) represents the exponential radial field dependence with altitude

With the change of variable $\mu r = s$, and the change of function $S(s) = R(s/\mu)$, Eq. (9.86b) is reshaped into the Bessel differential equation

$$s^2 d_{s^2}^2 S + s d_s S + \left(s^2 - m^2\right) S = 0, \tag{9.88}$$

with s also *a priori* a complex variable. The appropriate form of the solution and the values taken by μ are found when Eq. (9.88) is associated with boundary conditions at $s = 0$ and $s = \mu\rho$. This leads to a singular Sturm-Liouville problem because the coefficient of the second derivative vanishes at $s = 0$. Eq. (9.89) has two linearly independent solutions, the Bessel function of the first kind and integer order $J_m(s)$ and the Neumann function $N_m(s)$. However, the Neumann functions have to be discarded because they tend towards infinity when s tends towards 0, thus

$$R(r) = J_m(\mu r). \tag{9.89}$$

The factor μ can be specified by setting the boundary condition at $s = \mu\rho$. This writes

$$\alpha J_m(\mu\rho) + \beta J_m^{'}(\mu\rho) = 0. \tag{9.90}$$

The zeros of J_m and $J_m^{'}$ are real (Abramowitz and Stegun, 1965, section 9.5). In addition, if $\alpha = 0$ or $\beta = 0$, μ must be real but it may be shown that this remains true (in the general case) for any real value of α and β. Therefore, the variable s is real and μ is a root of the function $\alpha J_m(\mu\rho) + \beta J_m^{'}(\mu\rho)$. There are infinitely many values of μ which verify Eq. (9.90). They build up a countable subset of $\mathbb{R}$, depending on m and which can therefore be indexed by the pair (m, k) with $k \in \mathbb{N}^*$. Formally, the solution should write

$$\begin{aligned} V(r,\theta,z) = &\sum_{m=0}^{M}\sum_{k=0}^{K} J_m(\mu_{mk} r)\,(D_{mk}\cos m\theta \\ &+ E_{mk}\sin m\theta)\exp(\mu_{mk} z), \end{aligned} \tag{9.91}$$

and be a complete basis. In spite of these considerations, (Alldredge, 1982) adopted another form, with no definite boundary condition on the boundary $r = \rho$

$$\begin{aligned} V(r,\theta,z) = &Az + \sum_{m=0}^{M}\sum_{k=0}^{K} J_m(k\nu r)\,(D_{mk}\cos m\theta \\ &+ E_{mk}\sin m\theta)\exp(kz), \end{aligned} \tag{9.92}$$

with ν a scaling factor that is tuned manually and empirically by trials and errors.

Equation (9.92) is valid inside the cylinder, half-infinite towards negative z, apart from the linear term. Indices m are integers, as expected. In the formalism of Alldredge (1982), the choice of μ $(=k\nu)$ is not based upon boundary condition but on scale considerations. This raises some important practical difficulties illustrated by Fig. 9.6 that shows the CHA model obtained from the set of synthetic data Z_{all} using expression (Eq. 9.92) for the potential. After several tries, we could find a scaling parameter ν that allowed an apparent satisfying fit of the large scales of the magnetic field; there are certainly an infinite number of ν that would give comparable result. However, the same value of ν cannot represent both large and small scales and all crustal field contributions end up in the residual map. For some applications related to regional main field modelling, this low-pass property appears interesting as it seems to filter out crustal field contamination. This result is however misleading because the manual choice of ν act as a filter that has no real significance. By no means can we assert that the main field has been correctly represented because the set of functions do not form a complete basis; the residuals illustrate this incompleteness not a resolution problem imposed by the series truncation. The functions being not orthogonal, spectral analysis are not permitted and introducing multi-altitude data would have introduced other difficulties. As it stands, the CHA modelling is flawed. The mathematics would be correct after setting boundary conditions, at least on the lateral surface. They would define not one value of ν in Eq. (9.92) but a discrete set of μ_{mk} (Eq. 9.91) varying in m and k thus defining a complete basis function allowing the representation of any contribution of magnetic field (core and crustal) in the horizontal plane (dealing with multilevel data would require boundary conditions on the lower and upper surfaces).

9.4.2 SCHA and R-SCHA

Spherical Cap Harmonic Analysis and Revised Spherical Cap Harmonic Analysis are, in regional modelling, the closest relatives to SHA. SCHA was designed by Haines (1985a) to provide a reference field for Canada (Haines, 1985b). Since then, SCHA

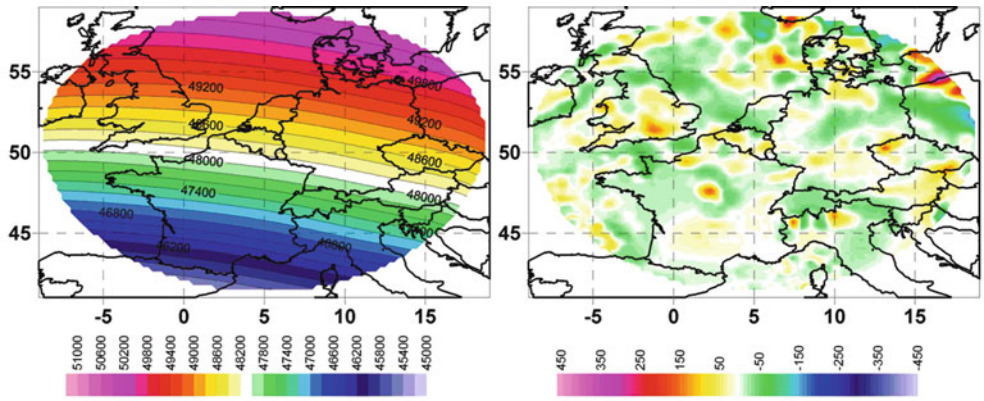

Fig. 9.6 Example of Cylindrical Harmonic Analysis using the Z vector component only. The obtained CHA model (*left*) and the residuals between the model and data (*right*) illustrate some of the properties discussed in the text. Units are in nT

has been widely used in a variety of regional models, including reference field models, secular variation, crustal field, external field, and even outside geomagnetism making it probably the most popular regional modelling method (see Torta et al., 2006, for a review).

9.4.2.1 Definition of the Domain

The domain of interest is shown on Fig. 9.7. It is the bounded volume Ω delimited by the intersection of a spherical shell $S(b, c)$ defined in Section (9.2), with a circular cone having its summit at the center of the Earth and aperture angle θ_0. The location of the cone axis and the half-angle θ_0 on the Earth depend of course on the area of interest. Generally, the radius of the inner sphere is the earth's mean radius (i.e., $b = R_E$ according to previous notations. We now set $R_E = a$ to avoid confusion with the radial function). The closed boundary $\partial\Omega$ of Ω consists in three pieces of geometrically simple boundaries: $\partial_{\theta_0}\Omega$ denotes the lateral portion of the cone $\theta = \theta_0$, $\partial_a\Omega$ and $\partial_c\Omega$ stand for the lower and upper cap at radii a and c respectively. Thus, the boundary $\partial\Omega = \partial_{\theta_0}\Omega \cup \partial_a\Omega \cup \partial_c\Omega$ is substantially more complicated than the boundary of the spherical shell.

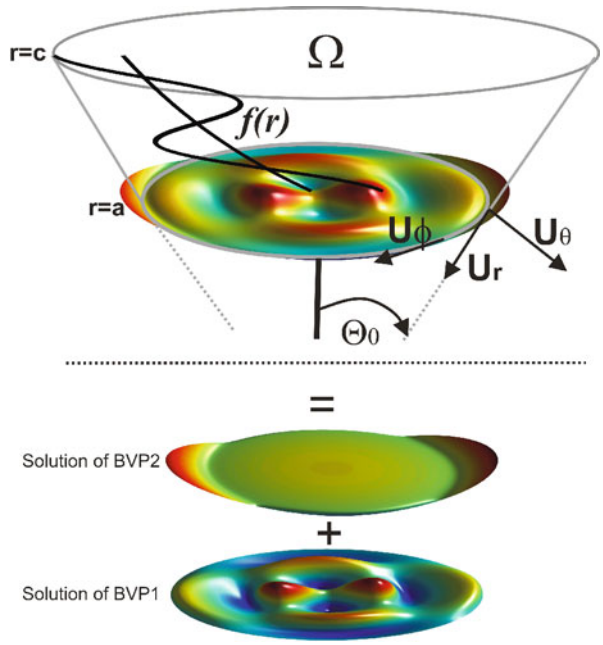

Fig. 9.7 Schematic representation of the spherical cone considered when solving a R-SCHA problem. The upper color surface (at $r = a$) represents the superimposition of the two independent solutions found when splitting the original BVP (Eq. 9.99) into two independent BVP's (Eq. 9.100 and 9.101). $f(r)$ represents the respective radial solution of BVP1 and BVP2 (see text for details)

9.4.2.2 Resolution of Laplace Equation in SCHA by the Fourier Decomposition Method

The resolution follows closely the pattern of Section (9.2.1). The only difference resides in the boundary conditions on Eq. (9.9). In SCHA, they are

$$P \text{ and } P' \text{ finite at } \theta = 0, \tag{9.93a}$$

$$\alpha P(\theta_0) + \beta P'(\theta_0) = 0. \tag{9.93b}$$

Instead of the mixed boundary condition defined in Eq. (9.93b), Haines (1985a) uses two separate

Dirichlet (with $\beta = 0$) and Neumann conditions (with $\alpha = 0$) and adds both sets of solutions. As already said above this non-orthodox procedure is applied with the hope to define a series expansion that convergences uniformly towards the solution. Here, for discussion purposes, we call SCHA the well-known solution of the Sturm-Liouville problem defined by Eq. (9.8) together with boundary conditions (9.93a) and (9.93b). We solve

$$\nabla^2 V = 0 \text{ on } \Omega, \tag{9.94a}$$

$$\alpha\,(V)_{\partial_{\theta_0}} + \beta \left(\frac{\partial V}{\partial n}\right)_{\partial_{\theta_0}} = 0. \tag{9.94b}$$

Note that in SCHA the Boundary Value Problem (BVP) is again incomplete as no condition is put on the boundary $\partial_a\Omega \cup \partial_c\Omega$. As was the case for RHA and CHA, there is no sufficient constraint on the radial function to ascertain that the solution will behave correctly with altitude. This, in turn, prevents us from dealing with multi-level data.

The solutions of Eq. (9.8), where the constant ν is *a priori* arbitrary, are the generalized Legendre functions (Hobson, 1965, Chapter V; Robin, 1958, Vol. II) of first (P_ν^m) and second (Q_ν^m) kind. As in SH, the condition expressed by (93a) excludes the second kind. The function P_ν^m is the eigenvector of the operator defined in Eq. (9.15). Thanks to the boundary conditions (9.93b), this operator is self-adjoint on the space $D = \{P \in L^2\,]u_0, 1[\,\cap\, C^2\,[u_0, 1],\ P$ fulfilling the boundary condition Eq. (9.93b)$\}$, where $u_0 = \cos\theta_0$. Therefore, the eigenvalues $\nu\,(\nu+1)$ are real. If, in addition, the constants α and β have the same sign (a condition obviously fulfilled with Dirichlet or Neumann conditions), the operator in Eq. (9.13) is positive (Reddy, 1998, section 6.5), which in turn implies that the eigenvalues $\nu\,(\nu+1)$ are real positive. The detailed resolution of the hypergeometric equation defined by Eq. (9.13) shows that $\nu > m$ if the boundary condition (93b) is also to be fulfilled. There is no loss of generality if we take ν real positive or null (with Neumann condition) since $P_\nu^m = P_{-\nu-1}^m$ (Robin, 1958, Vol. II, p.52). As in SH, the functions

$$\beta_k^m(\theta,\varphi) = P_{\nu(k,m)}^m(\cos\theta)e^{im\varphi}\ m \in \mathbb{Z}, \tag{9.95}$$

are eigenfunctions of $-\nabla_S^2$ associated to the eigenvalues $\nu\,(\nu+1)$ (in order to avoid unnecessary complications, we will hereafter discard the complex form because P_ν^m and P_ν^{-m} are connected to each other by a factor involving the gamma function — see Robin, 1958, Vol. II, p. 58). For simplicity we again keep the notation appropriate to the complex form. The constant function $\beta_0^0(\theta,\varphi)$ may or not be included into the set of basis functions, depending on the values taken by the coefficients α and β: if $\alpha = 0$ (Neumann boundary condition), $\beta_0^0(\theta,\varphi)$ fulfills the boundary condition and is therefore acceptable, but has to be discarded in all other cases.

The values of ν are the roots of the function $\alpha P_\nu^m(\theta_0) + \beta P_\nu'^m(\theta_0)$ and depend on m. The integer k indexes these roots for fixed m. Haines (1985a) showed how to compute them in the case of the Dirichlet or Neumann boundary conditions. The method applies likewise to the mixed boundary condition with some more numerical complexity. The general expressions of the basis functions are

$$\psi_{i,k}^m(r,\theta,\varphi) = a\left(\frac{a}{r}\right)^{\nu(m,k)+1}\beta_k^m, \tag{9.96a}$$

$$\psi_{e,k}^m(r,\theta,\varphi) = a\left(\frac{r}{a}\right)^{\nu(m,k)}\beta_k^m, \tag{9.96b}$$

and the potential simply writes

$$\begin{aligned} V(r,\theta,\varphi) = &\sum_{k=0}^{\infty}\sum_{m=0}^{\infty} G_k^{i,m}\psi_{i,k}^m(r,\theta,\varphi) \\ &+G_k^{e,m}\psi_{e,k}^m(r,\theta,\varphi). \end{aligned} \tag{9.97}$$

Such expressions look very similar to SH expansion (Eq. 9.18), which is misguiding. The degrees ν form a discrete set of real values depending on the order m. Therefore, the interpretation of the subscripts i and e in terms of truly inner and external field sources with respect to the sphere $S(a)$ is not as straightforward as in SH.

Despite its popularity and its apparently close relationship with SH, it was noticed by several authors (e.g., De Santis and Falcone, 1995) that it was difficult to model correctly the radial dependency, particularly when considering cones of small aperture (De Santis, 1991). This led some authors (Torta et al., 2006 for a review) to artificially increase the size of the cap (we understand now that this is done empirically to enforce the data to agree with the Neumann and Dirichlet conditions on the lateral surface). More intriguing, it was doubted that SCHA could simultaneously solve

for the horizontal and radial components with comparable accuracy (Langel and Hinze, 1998, p. 132; Thébault and Gaya-Piqué, 2008). In fact, troubles arise because the incomplete setting of the boundary value problem leads to an incomplete set of basis functions with respect to the relevant function space defined on Ω. Mathematically, it is sufficient to demonstrate the lack of completeness of SCHA by finding one single counter-example. The following Dirichlet problem

$$\nabla^2(V) = 0 \text{ on } \Omega \tag{9.98a}$$

$$V = f \text{ on } \partial_{\theta_0}\Omega \tag{9.98b}$$

$$V = 0 \text{ on } \partial_a\Omega \cup \partial_b\Omega, \tag{9.98c}$$

for instance, would have a null SCHA expansion on the spherical cap; the true solution being obviously not the null function.

Figure 9.8 illustrates one peculiarity of SCHA. We apply the original formalism of Haines (1985a) who, once more, introduces both bases derived from the Neumann and the Dirichlet boundary value problem. We use only the core field part of Z_{all} so that the data do not contain crustal field contributions. This helps us to illustrate the major deficiency of SCHA. The data are represented to 380 km wavelength only because reaching the 100 km spatial resolution was not possible (this resolution is reached in Fig. 9.2 and 9.4). The contradiction between the horizontal and vertical component, as well as non-orthogonality between basis functions, grew up so much that SCHA increasingly failed in representing the field and become more and more unstable. Since the data are equally distributed and dense, regularization based on minimum norm solution is helpless. It suggests that SCHA does not converge towards SH as it should do in the case of an infinite expansion (see also the above discussion about the lack of completeness of SCHA). Such problems are less prominent in many situations, when considering residual fields (even though they are proportional to the strength of the magnetic field, the model error may be of the order of the data noise and thus, discarded) or when considering very large caps.This latter case is better understood by noting that $\lim_{\theta_0 \to \pi/2} \nu(m,k) = n$, where n is an integer degree of SH; thus SCHA becomes an even closer relative to SH for large caps.

9.4.2.3 R-SCHA as a Boundary Value Problem

The Revised SCHA (R-SCHA) is a proposal that should remedy the drawback of SCHA (e.g., Thébault et al., 2004). We give here a general form of the complete boundary value problem. A general BVP, adapted to the domain Ω described in Section 9.4.2.1 and to the Laplace equation, would write (Reddy, 1998, section 8.3)

$$\nabla^2 V = 0 \text{ on } \Omega \tag{9.99a}$$

$$\alpha V + \beta \frac{\partial V}{\partial n} = G \text{ on } \partial\Omega = \partial_{\theta_0}\Omega \cup \partial_a\Omega \cup \partial_c\Omega, \tag{9.99b}$$

where α, β, G are given functions on $\partial\Omega$ (see Fig. 9.7). A first limitation arises if the BVP is to be resolved with the method of variable separation that requires α and β being constant on each piece $\partial_a\Omega$, $\partial_c\Omega$, $\partial_{\theta_0}\Omega$ of the closed surface $\partial\Omega$ but allows however these constants to be different on each piece. The method of variable separation requires in addition to split up the initial BVP into two simpler, partially homogeneous, independent BVP problems

$$\nabla^2 V_1 = 0 \text{ on } \Omega \tag{9.100a}$$

$$\frac{\alpha_{\theta_0}}{r} V_1 + \beta_{\theta_0} \frac{\partial V_1}{\partial n} = 0 \text{ on } \partial_{\theta_0}\Omega \tag{9.100b}$$

$$\alpha_a V_1 + \beta_a \frac{\partial V_1}{\partial n} = G_a \text{ on } \partial_a\Omega \tag{9.100c}$$

$$\alpha_c V_1 + \beta_c \frac{\partial V_1}{\partial n} = G_c \text{ on } \partial_c\Omega, \tag{9.100d}$$

$$\nabla^2 V_2 = 0 \text{ on } \Omega \tag{9.101a}$$

$$\frac{\alpha_{\theta_0}}{r} V_2 + \beta_{\theta_0} \frac{\partial V_2}{\partial n} = G_{\theta_0} \text{ on } \partial_{\theta_0}\Omega \tag{9.101b}$$

$$\alpha_a V_2 + \beta_a \frac{\partial V_2}{\partial n} = 0 \text{ on } \partial_a\Omega \tag{9.101c}$$

$$\alpha_c V_2 + \beta_c \frac{\partial V_2}{\partial n} = 0 \text{ on } \partial_c\Omega, \tag{9.101d}$$

where, for the sake of clarity, the function G has been subscripted according to the piece of boundary involved. Clearly, due to the linearity of the problem, the sum $V = V_1 + V_2$ is a solution of the initial BVP (Eq. 9.99). The BVP defined by the set of Eq. (9.100), (respectively Eq. 9.101), will be termed BVP1 (respectively BVP2) hereafter.

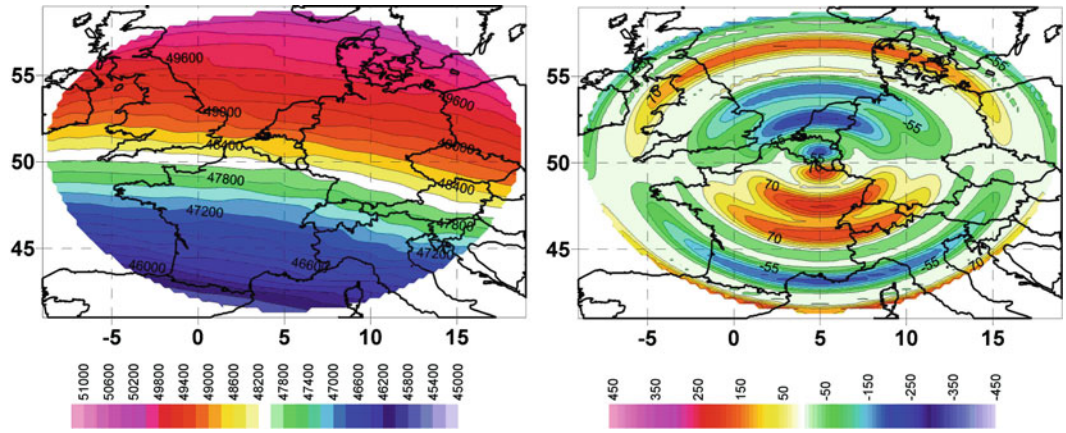

Fig. 9.8 Example of Spherical Cap Harmonic Analysis by least-squares inversion of the Z vector core component. The obtained SCHA model (*top-left*) and the residuals between the model and data (*top-right*) are discussed in the text

BVP1 was solved in Section 9.4.2.2 and will not be discussed any further. BVP2 was extensively discussed elsewhere in two particular cases: ($\alpha_{\theta_0} = \alpha_a = \alpha_c = 0$; Thébault et al., 2004) and ($\beta_{\theta_0} = \alpha_a = \alpha_c = 0$; Thébault et al., 2006a; 2006b). We thus limit ourselves to the changes inferred by the more general boundary conditions (101c and 101d). The most striking difference between BVP2 and the SCHA formulation (typically BVP1) is the Sturm-Liouville problem arising for the radial function $R(r)$ that writes

$$-d_r\left(r^2 d_r R(r)\right) = \lambda R(r) \text{ on }]a,c[\tag{9.102a}$$

$$\alpha_a R(a) - \beta_a R'(a) = 0 \tag{9.102b}$$

$$\alpha_c R(c) + \beta_c R'(c) = 0, \tag{9.102c}$$

Define $L^2(]a,c[)$ the Hilbert space on the interval $]a,c[$ endowed with the inner product $\langle f,g\rangle = \int_a^c f(r)g(r)dr$. The operator $D = -d_r\left(r^2 d_r\right)$ appearing on the left-hand side of (102a) is a particular case of a regular Sturm-Liouville operator that is self-adjoint on the space of the functions of $C^2([a,c]) \cap L^2(]a,c[)$ fulfilling conditions (Eq. 9.102b) and (Eq. 9.102c). Therefore, the eigenvalues λ are real. If, in addition, the pairs (α_a, β_a), (α_c, β_c) have the same sign, the operator is positive (i.e., $\langle D(f), f\rangle \geq 0$) and λ is real positive or null. This positivity property, which is not really important for our purpose, derives from the expression of D, which includes the minus sign, in accordance with the general form of a Sturm-Liouville operator (see Eq. 9.83). Note that the sign change in Eq. (9.102a) does not follow the convention adopted in Thébault et al., (2004, 2006a). The general solution of (102a) may be still formally written

$$R(r) = A_1\left(\frac{r}{a}\right)^{\nu} + A_2\left(\frac{a}{r}\right)^{\nu+1}, \tag{9.103}$$

with $\lambda = -\nu(\nu+1)$ when $\lambda \neq 1/4$, and

$$R(r) = \left(A_1 \ln\left(\frac{r}{a}\right) + A_2\right)\left(\frac{a}{r}\right)^{1/2}, \tag{9.104}$$

when $\lambda = 1/4$, that is when $\nu = -1/2$. As usual, the values of ν are such that the BVP2 (Eq. 102) has a non trivial null solution. They are the roots of an equation, which resolution relies upon approximate numerical methods in the general case. However, analytical solutions can be straightforwardly derived if we adopt more restrictive boundary conditions

$$a\frac{\alpha_a}{\beta_a} = -c\frac{\alpha_c}{\beta_c} = \alpha, \tag{9.105}$$

which assumes non zero values for β_a and β_c but includes the Neumann homogeneous boundary conditions ($\alpha_a = \alpha_c = 0$), when $\alpha = 0$, and

$$\frac{\beta_a}{a\alpha_a} = -\frac{\beta_b}{b\alpha_c} = \alpha, \tag{9.106}$$

which assumes non zero values for α_a and α_c but includes the homogeneous Dirichlet boundary conditions ($\beta_a = \beta_c = 0$) when $\alpha = 0$. Hereafter, the conditions defined in Eq. (9.105) (respectively Eq. 9.106) are referred to as case 1 (respectively case 2). Case 1 leads to eigenfunctions R_p, up to a multiplying constant given by

$$R_p(r) = \sqrt{\frac{a}{r}}\left[\frac{\pi p}{S(\alpha+1/2)}\cos\left(\frac{\pi p}{S}\ln\left(\frac{r}{a}\right)\right) + \sin\left(\frac{\pi p}{S}\ln\left(\frac{r}{a}\right)\right)\right], \tag{9.107}$$

that are associated to the eigenvalues

$$\lambda = \frac{1}{4} + \left(\frac{p\pi}{S}\right)^2 \quad p \in \mathbb{N}^*, \tag{9.108}$$

where $S = \ln(c/a)$, or eigenfunctions

$$R_\alpha(r) = \left(\frac{r}{a}\right)^\alpha, \tag{9.109}$$

associated to the eigenvalue $\lambda = -\alpha(\alpha+1)$, which is null if $\alpha = 0$ or $\alpha = -1$ and negative if $\alpha \notin]-1, 0[$. We note that there is only one possibly negative eigenvalue. Interestingly, the eigenfunction associated to the negative eigenvalue (i.e., for $\alpha \notin]-1, 0[$) have the same shape as the basis functions of BVP1 but verify nevertheless the boundary conditions of BVP2. Case 2 leads to eigenfunctions

$$R_p(r) = \sqrt{\frac{a}{r}}\left[\frac{\pi\alpha p}{S(1+\alpha/2)}\cos\left(\frac{\pi p}{S}\ln\left(\frac{r}{a}\right)\right) + \sin\left(\frac{\pi p}{S}\ln\left(\frac{r}{a}\right)\right)\right], \tag{9.110}$$

that are associated to the eigenvalues given by Eq. (9.108) or to

$$R(r) = \left(\frac{r}{a}\right)^{1/\alpha}, \tag{9.111}$$

associated to the possibly negative eigenvalue $\lambda = -\frac{1}{\alpha}\left(\frac{1}{\alpha}+1\right)$. In this last case, the complete solutions of BVP2 take again the form Eq. (9.96b) with ν (m, k) replaced by $1/\alpha$. Of course, this basis functions exist only in the case $\alpha \neq 0$. Let us summarize the shape of the solutions for the problem BVP2. In every case the basis functions may be written in the complex form

$$\psi_p^m(r,\theta,\varphi) = \gamma_p^m(r,\varphi)K_p^m(\cos\theta), \tag{9.112a}$$

$$\psi_\alpha^m(r,\theta,\varphi) = \gamma_\alpha^m(r,\varphi)P_\alpha^m(\cos\theta). \tag{9.112b}$$

The $\gamma_p^m(r,\varphi)$ and $\gamma_\alpha^{c,m}(r,\varphi)$ functions are defined by

$$\gamma_p^m(r,\varphi) = R_p(r)e^{im\varphi}; \gamma_\alpha^m(r,\varphi) = R_\alpha(r)e^{im\varphi} \quad \text{with } m \in \mathbb{N} \tag{9.113}$$

$K_p^m(\cos\theta)$ are the Mehler or conical functions described in Thébault et al. (2004, 2006a) (see also Gil et al., 2009 for a recent numerical discussion) and $P_\alpha^m(\cos\theta)$ generalized Legendre functions of real degree $P_\alpha^m(\cos\theta)$. As usual, the complex notation is kept for simplicity but we consider only real functions as solutions. The expressions of $R_p(r)$, $R_\alpha(r)$, eigenvalues λ and, hence, of $K_p^m(\cos\theta)$, $P_\alpha^m(\cos\theta)$, depend on the boundary conditions.

9.4.2.4 Orthogonality Properties, Uniqueness and Completeness

We now examine to which extent the orthogonality properties valid in SHA with respect to the inner product (Eq. 9.19) are valid for SCHA and R-SCHA functions. The orthogonality properties of $\psi_{i,k}^m$, and $\psi_{e,k}^m$ rely on those of $\beta_k^m(\theta,\varphi)$ (Eq. 9.95) on the spherical cap $S_{\theta_0}(1)$. The proofs were given by Lowes (1999). For R-SCHA, there is an extra complication with respect to SH due to the orthogonality properties of, and between, the basis functions $\psi_p^m(r,\theta,\varphi)$, $\psi_\alpha^m(r,\theta,\varphi)$ (see Eq. 9.112) as well as between these letters and family of functions ψ_k^m. Functions $\psi_p^m(r,\theta,\varphi)$ (or $\psi_\alpha^m(r,\theta,\varphi)$) are not orthogonal to each other with respect to the inner product defining $L^2(\Omega)$ because $R_p(r)$ and $R_{p'}(r)$ (Eq. 9.107 or Eq. 9.110) are orthogonal with respect to the inner product $\int_a^c R_p(r)R_{p'}(r)dr$ not with respect to $\int_a^c r^2 R_p(r)R_{p'}(r)dr$ as derived from Eq. (9.19). Orthogonality properties are restored if we resort to a weighted inner product and to a weighted Sobolev space $W^1(\Omega)$ defined

by the functions f on Ω possessing the properties: $\frac{f(\mathbf{r})}{(a^2+r^2)^{1/2}}$ and every partial derivative $\partial_{x_i}(f)$ belong to $L^2(\Omega)$ (Dautray and Lions, 1988, Chapter XI, p. 649). Knowing that on the domain Ω under consideration, $a \leq r \leq c$, the denominator $\left(a^2+r^2\right)^{1/2}$ may be equivalently replaced by r, $W^1(\Omega)$ is a Hilbert space for the following (real) inner product

$$\langle f, g\rangle_{W^1} = \int_\Omega \left[\frac{f(\mathbf{r})g(\mathbf{r})}{r^2} + \overrightarrow{\nabla} f \cdot \overrightarrow{\nabla} g\right] d\tau. \quad (9.114)$$

For the same reasons as for the SH analysis the subspace $W^1(\Omega)$ is not relevant for harmonic functions since the potential is not the measured quantity. It is thus judicious to define an inner product based only on the gradients. Thus, let us denote again $U(\Omega)$ the subspace of the harmonic functions of $W^1(\Omega)$ and provide $U(\Omega)$ with the inner product defined by Eq. (9.19). As it defines only a semi-norm, it is possible to put further constraints on $U(\Omega)$ in order to derive a true norm. We did not explore this possibility but leave it for future investigations.

The basis functions ψ_p^m, ψ_α^m (Eq. 9.112) are orthogonal with respect to the inner product (Eq. 9.114), both terms of the integrand being null. The same property holds true for each family of the basis functions $\psi_{i,k}^m(r,\theta,\varphi)$ and $\psi_{e,k}^m(r,\theta,\varphi)$, (Eq. 9.96) but not necessarily between the families. The orthogonality between the families of functions arising from BVP1 or BVP2, namely pairs like $(\psi_k^m, \psi_{p'}^{m'})$ are obviously holds true for $m \neq m'$ but we need to compute

$$I = \left\langle \psi_k^m, \psi_p^m \right\rangle_U = \int_\Omega \overrightarrow{\nabla} \psi_k^m \cdot \overrightarrow{\nabla} \psi_p^m d\tau. \quad (9.115)$$

Writing $\psi_k^m = \{\psi_{i,k}^m(r,\theta,\varphi), \quad \psi_{e,k}^m(r,\theta,\varphi)\}$ and using the Green identity Eq. (9.24), Eq. (9.115) may be transformed into

$$I = \int_{\partial\Omega} \psi_k^m \cdot \frac{\partial \psi_p^m}{\partial n} d\sigma = \int_{\partial_{\theta_0}\Omega} \frac{1}{r}\left(\partial_\theta \psi_p^m\right)_{\theta_0} \psi_k^m d\sigma - \int_{\partial_a\Omega} \left(\partial_r \psi_p^m\right)_a \psi_k^m d\sigma + \int_{\partial c\Omega} \left(\partial_r \psi_p^m\right)_c \psi_k^m d\sigma. \quad (9.116)$$

Taking the general form of the boundary conditions (9.100b), (9.101c), (9.101d) but restricting them to the particular forms $a\frac{\alpha_a}{\beta_a} = -c\frac{\alpha_c}{\beta_c} = \alpha_1$ or $\frac{\beta_a}{a\alpha_a} = -\frac{\beta c}{b\alpha_c} = \alpha_2$, it turns out that I vanishes only in the cases $(\alpha_1 = \beta_{\theta_0} = 0)$ or $(\alpha_2 = \alpha_{\theta_0} = 0)$. These conditions are respectively equivalent to $\left(\alpha_a = \alpha_c = \beta_{\theta_0} = 0\right)$, a Neumann condition on $\partial_a\Omega \cup \partial_b\Omega$ and a Dirichlet condition on $\partial_{\theta_0}\Omega$, and to $\left(\beta_a = \beta_c = \alpha_{\theta_0} = 0\right)$, a Dirichlet condition on $\partial_a\Omega \cup \partial_b\Omega$ and a Neumann condition on $\partial_{\theta_0}\Omega$. Conditions $\left(\beta_a = \beta_c = \alpha_{\theta_0} = 0\right)$ are hereafter denoted model M_1 and conditions $\left(\alpha_a = \alpha_c = \beta_{\theta_0} = 0\right)$ model M_2.

Considering a function V belonging to $U(\Omega)$, its expansion on the bases $\left\{\psi_{i,k}^m, \psi_{e,k}^m,\right\}$ and $\{\psi_p^m, \psi_\alpha^m\}$ is the sum of the following double series (Thébault et al., 2006a)

$$S_V = a\sum_{m=0}^{\infty}\sum_{k=1}^{\infty}\left(G_k^{i,m}\psi_{i,k}^m + G_k^{e,m}\psi_{e,k}^m\right) + a\sum_{m=0}^{\infty}\sum_{p=1}^{\infty}\left(G_p^m\psi_p^m\right) + a\sum_{m=0}^{\infty}\left(G_\alpha^m\psi_\alpha^m\right). \quad (9.117)$$

The gradients of V are orthogonal in Ω only in the cases described by M_1 and M_2. This provides a mean to estimate the Gauss coefficients separately by

$$\begin{aligned} G_k^{i,m}\left\|\psi_{i,k}^m\right\|_U^2 &= \left\langle V, \psi_{i,k}^m\right\rangle_U ; G_k^{e,m}\left\|\psi_{e,k}^m\right\|_U^2 = \left\langle V, \psi_{e,k}^m\right\rangle_U \\ G_p^m\left\|\psi_p^m\right\|_U^2 &= \left\langle V, \psi_p^m\right\rangle_U ; G_\alpha^m\left\|\psi_\alpha^m\right\|_U^2 = \langle V, \psi_\alpha^m\rangle_U, \end{aligned} \quad (9.118)$$

Equation (9.118) provides the essential argument against the ability of regional modelling technique to discriminate between internal and external magnetic fields with respect to the Earth's surface. Considering the expansion of V in SH (Eq. 9.28) is may be readily shown that setting $q_n^m = 0$ does not impose $G_k^{e,m} = 0$. This demonstrates that the "external" coefficients do not have the same meaning in SH and in R-SCHA formalisms. Regarding the completeness of R-SCHA expansion, the demonstration relies on the completeness of the bases β_k^m and γ_p^m on their respective spaces. The completeness is derived from the spectral properties of operators like ∇_S^2. Good accounts of the properties of this kind of operators may be found in Dautray and Lions (1988, Chapter VIII). R-SCHA is not designed to deal with single surface measurements. A good account of the ability of R-SCHA to process multi-level data is given in Thébault et al., (2006b).

9.4.3 Boundary Effects

Boundary effects, as already stated in Section (9.2.3), are closely related to uniform convergence (see Haines, 1990, for examples in one-dimensional spaces). Within the frame of generalized Fourier series, the boundary effects are nothing else than the expression of the Gibbs phenomenon, well-known and investigated at length in the case of the Fourier expansion of periodic functions. In this latter case, various summing methods may be used in order to accelerate the convergence rate and reduce the Gibbs effect (see for instance Robin, 1958, vol. II, Chapter VI, Hobson, 1965, Chapter VII, Jerri, 1998, section 3.5) which could probably be adapted in some cases in two dimensions (e.g., Thébault, 2006 who applied the Fejér partial sum theorem). Things are however a great deal more complicated with multi-dimensional series, more specifically with two-dimensional infinite series in the present case. Gonzalez-Velasco (1995, section 9.2) explored in details the case of harmonic expansion on a rectangular domain which involves periodic functions and showed, with a simple manageable example, how the complexity increases from the one-dimensional to two-dimensional situations. In particular, he stressed that uniform convergence depends on continuity property of the second mixed derivative ∂^2_{xy}. The difficulties are still enhanced in the case of SCHA and R-SCHA expansions due to the transcendental nature of the basis functions. Haines (1985a) claimed uniform convergence depending on consistency between the boundary conditions fulfilled by the basis functions and those verified by the potential to be approximated, referring to Sturm-Liouville theorem (see Section 9.4.1.1). This theorem is valid in the context of one-dimensional Sturm-Liouville problems only. To our knowledge, there is no extension to multi-dimensional problems, as illustrated by RHA and the two-dimensional ordinary Fourier series involved. Therefore, including both Neumann and Dirichlet conditions in SCHA does not even ensure a uniform convergence of the solution (but we admit that in practice they do converge faster).

Uniform convergence conditions have been set up for SH expansions. In that case, one may involve the first Harnack theorem mentioned in Section (9.2.3) (Kellog, 1929, p.248) which connects uniform convergence inside the domain to uniform convergence on its boundary. When the domain is a sphere or a shell, uniform convergence on the boundary relies on properties of Laplace series. The addition theorem of spherical harmonics allows transforming the two-dimensional series in degree l and order m into a one-dimensional series in l involving a Legendre expansion (see Kellog, 1929, chap. X and Hobson, 1965, chapter VII, for details). This is a mathematically well-founded simplification not possible in the case of SCHA or R-SCHA, although addition theorems exist for generalized Legendre functions (Hobson, 1965, chap. VIII, Robin, 1958, vol. III, chap. VII). According to Jerri (1998, Section 3.5), further investigations illustrating the link between rate of convergence and boundary conditions fulfilled by the potential to be approximated, could be carried out for instance with models M_1 and M_2 defined in the previous section. This investigation has not yet been performed.

9.4.4 Infinite Conical Domain

We define the infinite conical domain Ω_∞ as the domain described in Section (9.4.2.1) bounded by a sphere of infinite radius c. In order to investigate the changes brought to the expression of the basis functions for the bounded domain, we solve the following boundary value problem which is similar to problem M_2 defined in Section (9.4.2.4)

$$\nabla^2 (V) = 0 \text{ on } \Omega_\infty \tag{9.119a}$$

$$V = G_{\theta_0}(r, \varphi) \text{ on } \partial_{\theta_0}\Omega_\infty \tag{9.119b}$$

$$\frac{\partial V}{\partial n} = G_a(\theta, \varphi) \text{ on } \partial_a\Omega_\infty \tag{9.119c}$$

$$V \text{ and } \overrightarrow{\nabla} V \longrightarrow 0 \text{ when } r \to \infty. \tag{9.119d}$$

The problem is again split up into two subproblems with partially homogeneous boundary conditions (compare to Eqs. 9.100 and 9.101)

$$\nabla^2 V_1 = 0 \text{ on } \Omega_\infty \tag{9.120a}$$

$$V_1 = 0 \text{ on } \partial_{\theta_0}\Omega \tag{9.120b}$$

$$\frac{\partial V_1}{\partial n} = G_a \text{ on } \partial_a\Omega \tag{9.120c}$$

$$V_1 \text{ and } \overrightarrow{\nabla} V_1 \longrightarrow 0 \text{ when } r \to \infty, \tag{9.120d}$$

$$\nabla^2 V_2 = 0 \text{ on } \Omega_\infty \tag{9.121a}$$

$$V_2 = G_{\theta_0} \text{ on } \partial_{\theta_0}\Omega_\infty \tag{9.121b}$$

$$\frac{\partial V_2}{\partial n} = 0 \text{ on } \partial_a \Omega_\infty \tag{9.121c}$$

$$V_2 \text{ and } \overrightarrow{\nabla} V_2 \longrightarrow 0 \text{ when } r \to \infty. \tag{9.121d}$$

Basis functions derived from BVP (Eqs. 9.120) are the same as those of the BVP (Eqs. 9.100) except for the functions $\psi^m_{e,k}$ (Eq. 9.96b) which do not vanish at infinity and have therefore to be discarded. The main difference with the case of the bounded domain comes from the solutions of the second BVP (Eq. 9.121) and more specifically from the changes in Eq. (9.102) which now writes

$$-d_r\left(r^2 d_r R(r)\right) = \lambda R(r) \text{ on }]a, \infty[\tag{9.122}$$

$$R'(a) = 0 \tag{9.123}$$

$$R(r) \text{ and } R'(r) \to 0 \text{ when } r \to \infty. \tag{9.124}$$

It turns out that the eigenvalues are no longer a discrete set of complex numbers. They build up a continuum of the form

$$\lambda = \frac{1}{4} + y^2 = \nu\,(\nu + 1)\,, \tag{9.125}$$

where y is a real number, positive or null and the roots ν write

$$\nu = -\frac{1}{2} + y \text{ with } \; y \geqslant 0. \tag{9.126}$$

The radial functions, denoted $R_y\,(r)$, take the form

$$R_y(r) = \sqrt{\frac{a}{r}}\left[2y\cos\left(y\ln\frac{r}{a}\right) + \sin\left(y\ln\frac{r}{a}\right)\right] \quad \text{when } y > 0, \tag{9.127a}$$

$$\text{and } R_y(r) = \sqrt{\frac{a}{r}}\left[\ln\frac{r}{a} + 2\right] \quad \text{when } y = 0, \tag{9.127b}$$

The basis functions, equivalent to those given by Eq. (9.112a), write now

$$\psi^m_y\,(r, \theta, \varphi) = \gamma^m_y(r, \varphi) K^m_y(\cos\theta), \tag{9.128}$$

with

$$\gamma^m_y(r, \varphi) = R_y(r) e^{im\varphi} \quad m \in \mathbb{N}, \tag{9.129}$$

where the complex form, as before, is kept for simplicity. In the particular case $y = 0$, the Mehler function K^m_y may be more clearly written $P^m_{-1/2}$ which is a particular generalized Legendre function with real degree.

Splitting the exponential form of the φ-function into real-valued trigonometric function, the Fourier-like expansion of a potential V on the basis functions ψ^m_y more explicitly writes

$$S_V = a\sum_{m=0}^{\infty}\left[\cos m\varphi \int_{y=0}^{\infty} G^m\,(y)\, R_y(r) K^m_y(\cos\theta) dy + \sin m\varphi \int_{y=0}^{\infty} H^m\,(y)\, R_y(r) K^m_y(\cos\theta) dy\right]. \tag{9.130}$$

The integral factors are the equivalent of inverse Fourier transforms, the coefficients $G^m\,(y)$ and $H^m\,(y)$ being now functions of the real variable y instead of being indexed terms of a series. Thus, the formalism for the infinite cone is derived from that of the bounded cone in very much the same way as the Fourier transform may be derived from the ordinary Fourier series when the periodic interval is stretched out to infinity. The functions $G^m\,(y)$ and $H^m\,(y)$ might thus be interpreted as generalized Fourier transforms of the potential V. The space $U\,(\Omega)$ mentioned in Section (9.4.2.4) is still the functional frame. However, the domain being now unbounded, some care must be taken regarding the existence of the inner products $\langle f, g\rangle$ defined by Eq. (9.114) and $\langle f, g\rangle_U = \int\limits_{\Omega_\infty}\left(\overrightarrow{\nabla} f \cdot \overrightarrow{\nabla} g\right) d\tau$. Likewise, care must be exercised in the use of Green's identity (Eq. 9.24). The computation of $G^m\,(y)$ and $H^m\,(y)$ is alike the bounded case if the basis functions are still orthogonal with respect to

the inner product $\langle \cdot, \cdot \rangle_U$. Assuming that Green' identity holds true, we have

$$\left\langle \psi_y^m, \psi_{y'}^{m'} \right\rangle_U = \int\limits_{\partial_{\theta_0}\Omega_\infty} \psi_y^m \left(\frac{\partial \psi_{y'}^{m'}}{\partial n} \right)_{\partial_{\theta_0}\Omega_\infty} \sin\theta_0 r dr d\varphi \tag{9.131a}$$

$$= \delta_{m,m'} \left(1 + \delta_{m,0}\right) \pi \sin\theta_0 K_y^m(\theta_0) \partial_{\theta_0} \left(K_y^m\right) \int\limits_a^\infty R_y(r) R_{y'}(r) dr, \tag{9.131b}$$

where $\delta_{m,m'}$, $\delta_{m,0}$ are the Kronecker symbols. It may be shown, using the Fourier transform of the Heaviside function that

$$\int\limits_a^\infty R_y(r) R_{y'}(r)\, dr = 2\pi a (yy' + \frac{1}{4}) \delta\left(y - y'\right), \tag{9.132}$$

where $\delta\left(y\right)$ is the Dirac distribution. Thus, ψ_y^m, $\psi_{y'}^m$ are orthogonal in the generalized sense defined by Eq. (9.132). On the other hand, ψ_y^m and $\psi_{i,k}^m$ are still orthogonal due to the boundary conditions (Eqs. 9.120 and 9.121) they respectively fulfill. Taking into account the orthogonality property expressed by Eq. (9.132), it is now straightforward to compute $G^m\left(y\right)$ and $H^m\left(y\right)$. For instance

$$G^m\left(y\right) = \frac{\sin\theta_0 d_{\theta_0}\left(K_y^m\right)}{a \left\| R_y K_y^m \cos m\varphi \right\|_U^2} \int\limits_a^\infty R_y(r) dr \int\limits_0^{2\pi} V(r, \theta_0, \varphi) \cos m\varphi d\varphi. \tag{9.133}$$

Thébault (2008) used an hybrid variant of this method to construct a time-varying magnetic field model over France for the epochs between 1965 and 2007.5, restricting the expansion on the ψ_y^m to the only term $y = 0$ as this term at least was necessary in order to comply with basic properties of the magnetic field, and keeping the so-called external basis function in order to balance the incompleteness induced by this restriction. Therefore, the basis function corresponding to this latter approximation is, strictly speaking, not complete.

Figure 9.9 displays an application of the infinite cone restricting the expansion (Eq. 9.130) to $y = 0$ that is referred to as R-SCHA2D. The maximum series expansion in Eqs. (9.96a) and (9.96b) are defined to resolve the Z_{all} data to 100 km wavelengths. The model fits Z_{all} correctly both for the main and crustal fields. Part of the residuals are due to wavelengths smaller than 100 km but one can see the presence of circular edge effects near the Southern boundary. This is mostly caused by the choice of the Dirichlet boundary condition set in Eq. (9.120b) that makes the Z component converge slower than the horizontal component but the restriction to $y = 0$ may likely be responsible for some part of the residuals. Since the basis functions are orthogonal we could, in principle, compute a power spectrum (which does not make sense in case of aliasing). The total field can be fairly well represented but we cannot ascertain that the upward/downward continuation will be stable, unless we deal with magnetic fields with very specific properties, because the restriction to $y = 0$ may very well hold at the data surface but not anymore at another radius.

9.4.5 Slepian Functions

We now finish our overview of regional modelling with the Slepian functions. These functions originate from a problem in information theory, dealing with the optimal concentration of a signal in both the time and frequency domains (see Simons et al., 2006, for references). They may be introduced in two ways. First, by adopting the viewpoint of strictly band-limited functions (up to degree L in terms of spherical harmonics) which is an approach comparable to the SH expansion. Second, by making use of the concept of strictly spatially localized functions, which is closer to regional modelling like SCHA and R-SCHA. We restrict ourselves to the first approach, which takes a simple algebraic form, part of which has already been seen in the above paragraphs.

Let be H_L the space defined in Section (9.3.2) and $K_L\left(\rho\right)$ the subspace of $L^2\left(S_\rho\right)$ of the band-limited spherical harmonic functions defined on the sphere $S\left(\rho\right)$ ($\rho = R_E$ or simply r). $L^2\left(S_\rho\right)$ is endowed with the inner product defined in Eq. (9.16). H_L and $K_L\left(\rho\right)$ have the same dimension, namely $L\left(L+2\right)$. The functions $\psi_l^m\left(R\widehat{\mathbf{r}}\right)$ are identical to $\beta_l^m\left(\widehat{\mathbf{r}}\right)$ and are therefore orthonormal on $K_L\left(R\right)$, whereas $\psi_l^m\left(r\widehat{\mathbf{r}}\right)$ are orthogonal on $K_L\left(r\right)$ (see Eq. 9.18a for the definition of ψ_l^m -the subscript i having been dropped).

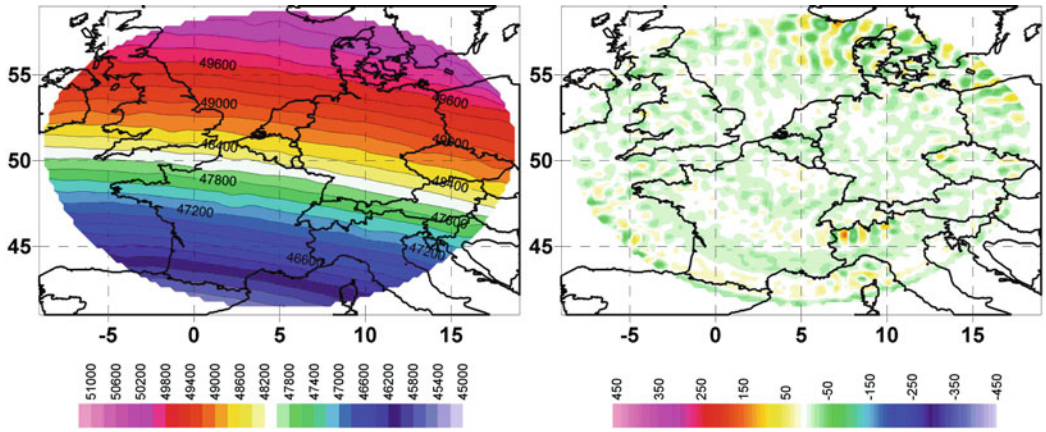

Fig. 9.9 Modelling of the magnetic field and the crustal field using an approximate expansion resembling to the solution of the infinite cone. This approach is called R-SCHA2D. On the left are shown the residuals. Units are in nT

As in Section (9.3.1.2), we illustrate the Slepian technique with the expression of the radial component rB_r. According to Eq. (9.52) and (9.53), where the maximum degree is L, the components $rB_{L,r}(r\widehat{\mathbf{r}})$ and $RB_{L,R}(R\widehat{\mathbf{r}})$ write

$$rB_{L,r}(r\widehat{\mathbf{r}}) = R\sum_{lm}^{L} p_l^m \psi_l^m(r\widehat{\mathbf{r}}) = R\sum_{lm}^{L} p_l^m(r)\, Y_{R,l}^m(R\widehat{\mathbf{r}}), \tag{9.134a}$$

$$RB_{L,R}(R\widehat{\mathbf{r}}) = R\sum_{lm}^{L} p_l^m \psi_l^m(R\widehat{\mathbf{r}}) = R\sum_{lm}^{L} p_l^m Y_{R,l}^m(R\widehat{\mathbf{r}}), \tag{9.134b}$$

with

$$p_l^m(r) = \left(\frac{R}{r}\right)^{l+1}(l+1)\, g_l^m = \left(\frac{R}{r}\right)^{l+1} p_l^m. \tag{9.135}$$

We define $Y_{R,l}^m(R\widehat{\mathbf{r}})$ as in Eq. (9.57) in order to better stress that they are functions defined on S_R. The expression $\sum_{lm}^{L}$ hereafter stands for $\sum_{l=1}^{L}\sum_{m=-l}^{l}$ according to the convention adopted by Simons and Dahlen (2006). The relation between $rB_{L,r}(r\widehat{\mathbf{r}})$ and $RB_{L,R}(R\widehat{\mathbf{r}})$ expanded in terms of the SH $Y_{R,l}^m(R\widehat{\mathbf{r}})$, hence the upward and downward continuation, has been discussed in (section 9.3.1.2).

9.4.5.1 Slepian Functions in $K_L(R)$

We are now looking for a set of basis functions of $K_L(R)$ localized in a region $\Sigma_R \subset S_R$. These functions, defined as $g(\widehat{\mathbf{r}})$, maximize the space energy ratio (Simons et al., 2006; Simons and Dahlen, 2006)

$$\lambda = \frac{\int_{\Sigma_R}\left[g(R\widehat{\mathbf{r}})\right]^2 d\sigma}{\int_{S_R}\left[g(R\widehat{\mathbf{r}})\right]^2 d\sigma}. \tag{9.136}$$

As g belong to $K_L(R)$, there are at most $L(L+2)$ linearly independent functions. Their expansion on the basis $\left\{Y_{R,l}^m\right\}$ writes

$$g_k(R\widehat{\mathbf{r}}) = \sum_{lm}^{L} \gamma_{l,k}^m Y_{R,l}^m(R\widehat{\mathbf{r}}). \tag{9.137}$$

For simplicity, the double indices (l,m) are mapped to a single index j according to the rule

$$j(l,m) = l^2 + l + m, \tag{9.138}$$

and the coefficients $\gamma_{l,k}^m$ can be written C_{jk}, $j = 1,\ldots,L(L+2)$. The column vector $\Gamma_k = C_{\cdot,k}$ belonging to $\mathbb{R}^{L(L+2)}$ contains the components of the vector $g_k(R\widehat{\mathbf{r}})$ on the basis $\left\{Y_{R,l}^m(R\widehat{\mathbf{r}})\ \text{or}\ Y_{R,j}(R\widehat{\mathbf{r}})\right\}$. Using the mapping from $K_L(R)$ onto $\mathbb{R}^{L(L+2)}$ just described, Simons et al. (2006) showed that the vectors Γ_k are the eigenvectors of the algebraic eigenvalue problem

$$\mathbf{D}(\Gamma) = \lambda\Gamma, \tag{9.139}$$

where $\mathbf{D}$ is the $L(L+2) \times L(L+2)$ — dimensional matrix whose elements are given by

$$D_{lm,l'm'} = \frac{1}{4\pi} \int_{\Sigma_1} Y_{R,l}^{m} (R\hat{\mathbf{r}})\, Y_{R,l'}^{m'} (R\hat{\mathbf{r}})\, d\sigma. \tag{9.140}$$

Σ_1 is the radial projection of Σ_R onto S_1. According to the mapping defined by Eq. (9.138), the elements of $\mathbf{D}$ may be indexed D_{ij}, $i = 1, \ldots, L(L+2)$, $j = 1, \ldots, L(L+2)$. $\mathbf{D}$ is the matrix of a symmetric (i.e., self-adjoint), positive operator on $\mathbb{R}^{L(L+2)}$, which range is $\mathbb{R}^{L(L+2)}$. Hence, there are $L(L+2)$ positive eigenvalues λ_k, associated to $L(L+2)$ orthogonal eigenvectors Γ_k whose components are $\left(C_{i,k}\right)_{i=1,\ldots,L(L+2)} = \left(\gamma_{l,k}^{m}\right)$. These eigenvectors may be normalized. Hence, the columns of the matrix $\mathbf{C}$ verify the property

$$\sum_{\alpha=1}^{L(L+2)} C_{\alpha j} C_{\alpha k} = \sum_{lm}^{L} \gamma_{l,j}^{m} \gamma_{l,k}^{m} = \delta_{jk}, \tag{9.141}$$

and the matrix $\mathbf{C}$ maps the basis $\left\{Y_{R,l}^{m}\right\}$ onto the basis $\{g_k\}$

$$g_k (R\hat{\mathbf{r}}) = \sum_{j=1}^{L(L+2)} C_{kj}^{T} Y_{R,j} (R\hat{\mathbf{r}}), \tag{9.142}$$

where $\boldsymbol{C}$ is an unitary matrix and therefore $\mathbf{C}^{-1} = \mathbf{C}^{T}$. Conversely

$$\begin{aligned} Y_{R,j} (R\hat{\mathbf{r}}) &= \sum_{k=1}^{L(L+2)} C_{jk} g_k (R\hat{\mathbf{r}}) \quad \text{or} \quad Y_{R,l}^{m} (R\hat{\mathbf{r}}) \\ &= \sum_{k=1}^{L(L+2)} \gamma_{l,k}^{m} g_k (R\hat{\mathbf{r}}). \end{aligned} \tag{9.143}$$

Thus, the Slepian functions are constructed such as to verify the property

$$\frac{1}{4\pi} \int_{S_1} g_j (R\hat{\mathbf{r}})\, g_k (R\hat{\mathbf{r}})\, d\sigma = \delta_{jk}. \tag{9.144}$$

In addition, they have the nice property of being likewise orthogonal on the region Σ_R (Simons and Dahlen, 2006)

$$\frac{1}{4\pi} \int_{\Sigma_1} g_j (R\hat{\mathbf{r}})\, g_k (R\hat{\mathbf{r}})\, d\sigma = \lambda_j \delta_{jk}. \tag{9.145}$$

As one may conjecture, this property plays a central role in the inverse problem. As expected, when Σ_R tends to cover the whole sphere, every eigenvalue tends towards 1 and $g_k (R\hat{\mathbf{r}})$ tends towards $Y_{R,l}^{m} (R\hat{\mathbf{r}})$. Technical details about the actual calculation of the Slepian functions are to be found in Simons et al. (2006). They show in particular that the mathematics are definitely simpler if Σ_1 is a circular cap. The component $RB_{L,R} (R\hat{\mathbf{r}})$ which expansion on the basis $\left\{Y_{R,l}^{m} (R\hat{\mathbf{r}})\right\}$ is given by Eq. (9.134b) may be likewise expanded on the basis $\{g_k (R\hat{\mathbf{r}})\}$

$$RB_{L,R} (R\hat{\mathbf{r}}) = R \sum_{k=1}^{L(L+2)} s_k g_k (R\hat{\mathbf{r}}). \tag{9.146}$$

According to the well-known algebraic rules for basis change, s_k and p_l^m are linked by

$$s_k = \sum_{j=1}^{L(L+2)} C_{jk} p_j = \sum_{lm}^{L} \gamma_{l,k}^{m} p_l^m, \tag{9.147a}$$

$$p_j = \sum_{k=1}^{L(L+2)} C_{jk} s_k \text{ or } p_l^m = \sum_{k=1}^{L(L+2)} \gamma_{l,k}^{m} s_k. \tag{9.147b}$$

9.4.5.2 Slepian Functions in $K_L(r)$

In order to calculate $rB_{L,r} (r\hat{\mathbf{r}})$, which expression in terms of solid spherical harmonics is given by Eq (9.134a), we may search likewise an expansion using the functions $g_k (R\hat{\mathbf{r}})$. Therefore $rB_{L,r} (r\hat{\mathbf{r}})$ writes

$$rB_{L,r} (r\hat{\mathbf{r}}) = R \sum_{k=1}^{L(L+2)} s_k (r)\, g_k (R\hat{\mathbf{r}}). \tag{9.148}$$

The functions $s_k (r)\, g_k (R\hat{\mathbf{r}})$ are orthogonal with respect to the inner product defined in Eq. (9.16) on the space $L^2 (S_r)$. This property guarantees the uniqueness of the

functions $s_k(r)$. Let us calculate them in terms of the constant p_l^m. We obtain

$$s_k(r) = \sum_{lm}^{L} \gamma_{l,k}^m p_l^m \left(\frac{R}{r}\right)^{l+1}, \tag{9.149}$$

which shows that the radial functions $s_k(r)$ are significantly more complicated than the $p_l^m(r)$ defined in Eq. (9.135). This will require that multi-level data have to be modelled with different functions $s_k(r)$. In order to write $s_k(r)$ in terms of $s_k(R)$, we replace p_l^m by its expression given by Eq. (9.147b)

$$s_k(r) = \sum_{j=1}^{L(L+2)} \left[\sum_{lm}^{L} \gamma_{l,k}^m \gamma_{l,j}^m \left(\frac{R}{r}\right)^{l+1}\right] s_j. \tag{9.150}$$

9.4.5.3 Potential Field Estimation On Σ_r

Let us turn back to the eigenvalues λ_k of Eq. (9.136). They are clearly in the interval $[0, 1]$. The largest values correspond to the Slepian functions most concentrated in the area Σ_R or equivalently Σ_r. The so-called "spherical Shannon number" defined by (Simons and Dahlen, 2006)

$$N = \sum_{k=1}^{L(L+1)} \lambda_k = (L+1)^2 \frac{A}{4\pi}, \tag{9.151}$$

where A is the area of Σ_R divided by R^2, provides an estimate of the number of Slepian functions to be retained in the expansion. The reduction of basis functions according to the eigenvalue magnitude, together with the property expressed by Eq. (9.145) makes the Slepian basis attractive for the inverse problem. We illustrate this point by considering the inverse problem consisting in estimating the coefficients $s_k(r)$ knowing rB_r $(= rB_{r,\text{mes}})$ on Σ_r. As usual, in the least-squares approach, we minimize a functional with respect to the coefficients $s_k(r)$ of the expansion given by Eq. (9.148). In the present case, the functional writes

$$d^2 = \frac{1}{4\pi r^2} \int_{\Sigma_r} \left[rB_{L,r}(r\widehat{\mathbf{r}}) - rB_{r,\text{mes}}(r\widehat{\mathbf{r}})\right]^2 r^2 d\sigma. \tag{9.152}$$

In practice, it is advisable to use a truncated sum. The Shannon number gives an indication of how to select the minimal eigenvalue but other choices may be made (see Simons and Dahlen, 2006 for a discussion) and therefore, we write J the maximal index (therefore, λ_J is the smallest eigenvalue). Replacing $rB_{L,r}(r\widehat{\mathbf{r}})$ by the truncated expansion, we obtain

$$\begin{aligned} d^2 = {} & \tfrac{R^2}{4\pi} \sum_{j=1}^{J}\sum_{k=1}^{J} s_j(r)\, s_k(r) \int_{\Sigma_1} g_j(R\widehat{\mathbf{r}})\, g_k(R\widehat{\mathbf{r}})\, d\sigma \\ & - \tfrac{2Rr}{4\pi} \sum_{j=1}^{J} s_j(r) \int_{\Sigma_1} g_j(R\widehat{\mathbf{r}})\, B_{r,\text{mes}}(r\widehat{\mathbf{r}})\, d\sigma \\ & + \tfrac{r^2}{4\pi} \int_{\Sigma_1} \left(B_{r,\text{mes}}(r\widehat{\mathbf{r}})\right)^2 d\sigma. \end{aligned} \tag{9.153}$$

Taking into account Eq. (9.145), d^2 becomes

$$\begin{aligned} d^2 = {} & R^2 \sum_{j=1}^{J} \lambda_j \left(s_j(r)\right)^2 - \frac{2Rr}{4\pi} \sum_{j=1}^{J} s_j(r) \int_{\Sigma_1} g_j(R\widehat{\mathbf{r}}) \\ & B_{r,\text{mes}}(r\widehat{\mathbf{r}})\, d\sigma + \frac{r^2}{4\pi} \int_{\Sigma_1} \left(B_{r,\text{mes}}(r\widehat{\mathbf{r}})\right)^2 d\sigma. \end{aligned} \tag{9.154}$$

The normal equations write

$$\lambda_j s_j(r) = \frac{1}{4\pi} \left(\frac{r}{R}\right) \int_{\Sigma_1} g_j(R\widehat{\mathbf{r}})\, B_{r,\text{mes}}(r\widehat{\mathbf{r}})\, d\sigma. \tag{9.155}$$

Equation (9.155) shows clearly the importance of the property expressed by Eq. (9.145) and of a good selection of the eigenvalue and Slepian eigenfunction set. Of course, this presentation is a rather elementary approach to the inverse problem. The reader is referred to Simons and Dahlen (2006) for further developments and to Simons et al. (2009) for an application to the modelling of the Bangui anomaly.

Figure (9.10) shows the residuals between the SH synthetic data Z_{all} and the Slepian reconstruction to $L = 200$. Note its similarity with Figures (9.9-right) and (9.2). The Slepians do rather well in reconstructing the total field in this case. Some subtleties are worth being mentioned. First, the Slepian reconstruction was performed here within a spherical cap but this is not required. Among the methods presented so far, this flexibility is rather unique and allows adjusting a model to very specific geometry (that is in general imposed by the available data distribution often correlated with the boundaries of countries). Second, the inverse problem is numerically well conditioned

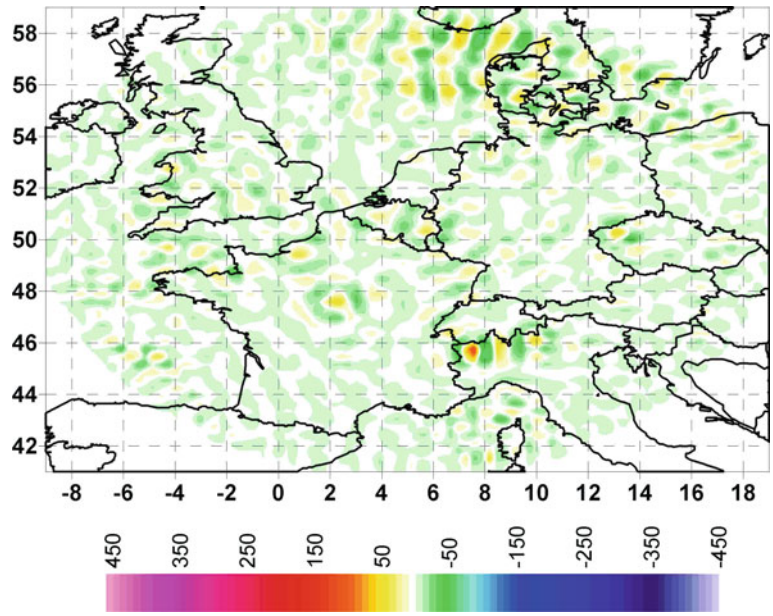

Fig. 9.10 Residuals in nT between the Z_{all} synthetic data and the slepian reconstruction using L = 200

thanks to the orthogonality of the Slepian functions and this allows estimating power spectra (Simons, 2010). Note, however, that a good *a priori* knowledge on the data error is required to avoid modelling the noise and select the optimal number of Slepian functions. At last, by virtue of Eq. (9.145) and its associated comments, Slepian functions are currently powerful for spectral analysis of surface collocated data but efforts are being made towards implementing the technique in order to process simultaneously the three components of the magnetic field vector data measured at different altitudes (Beggan and Simons, 2009).

9.5 Conclusions

We presented in a formal manner different techniques under development for modelling the Earth's magnetic field with, in its wide acceptation, local functions. We showed that the methods based on functions with global support are in fact different realizations of a unique expression given by Eqs. (9.37) and (9.38); they will then differ according to the chosen kernel and regularization. We then illustrated that most approaches provide similar result when a sufficiently large set of perfect magnetic field data at a single surface is available. The techniques are, however, not equivalent from a practical point of view when moving away from this ideal situation. The differences come up because the approaches discussed rely on sometimes fundamentally different concepts. Some do not necessarily solve Laplace equation (techniques inherited from signal processing, for instance), others do not converge uniformly (regional modelling without the appropriate boundary conditions) and, in general, none of them allow internal/external field separation (when applied over a portion of the sphere only). Methods with global support are arguably ill suited for dealing with magnetic field signals with local characteristics but are likely to allow internal/external field separation when they are applied at the global scale since they encompass the internal magnetic field sources of the Earth. Conversely, we do not see how regional modelling could be superior to SH for representing the large-scale fields (unless there is a data distribution issue, of course) because the lateral boundaries may introduce convergence difficulties such as Gibbs phenomenon. Roughly speaking, regional or global approaches thus require signals with wavelengths consistent with the dimension of the studied region. It does not mean that they will fail but that they will necessitate incorporating *a priori* information and regularization.

As one can realize by the preceding pages none of the technique is user-friendly. They require time of

adaptation and sometimes new coding from scratch. Understanding the groundwork of each philosophy first (global or regional support), then of each approach, to be able to pick up the technique the most relevant with respect to a particular magnetic dataset is a tedious work that explains well why local functions have not been more widely adopted so far even though they are, in principle, dedicated to detecting small-scale features detection that would be otherwise smoothed out in SH. Other difficulties, not detailed here, arise due to the real data accuracy, distribution of noise, artefacts or biases that require a specific expertise.

Yet, we argue that developing these techniques in the framework of geomagnetism is worth the effort, at least for two simple reasons. One is practical as in the forthcoming years a significantly large amount of high quality satellite data will complement the already large available dataset (Friis-Christensen et al., 2006). However, the amount of near-surface data will not grow as rapidly and the issue of near-surface data spatial distribution will remain critical. In addition, we should not forget that potential fields, in particular magnetic fields, are ones of the few remotely accessible internal properties in planetary explorations. Among some planetary magnetic fields, at least for the Moon and Mars, the contribution from the crust and thus small scales dominate other internal field contributions (e.g., Langlais et al., 2009). Local analysis should be there particularly effective. The second reason is to our point of view too often overlooked. The temptation is big to evaluate, or validate, the robustness of a regional model by comparing results with those provided by SH models. It is customary to prejudge that SH are more or less robust because models indeed showed remarkable fidelity over the last years, especially for the lithospheric field. One should keep in mind, however, that the similarities obtained between SH models may also reflect the self-consistency of the SH procedure (including the data processing) rather than the physics of the magnetic field. Early models of lithospheric fields in SH, based on different procedures, are in fact different (Thébault et al., 2010). In that respect, regional schemes may also be used to challenge the robustness of the standard SH models, to assess regionally their compatibility with dense near-surface measurements, and to verify that magnetic field features are indeed not bound to one specific way of representing the data.

Regional modelling is in its infancy and we do not have the necessary hindsight to state the context in which it is unquestionably superior to SH. Until now regional models have been generally presented as prototypes or used simply for mapping the magnetic field at national scales. Little serious work has been carried out regarding the possible significance of the residuals obtained between their results and equivalent SH models. Investigating if the mismatches show persistent features, if they are independent from the local method used and if they contain time-variability or even periodicity, etc. is ultimately a scope of regional modelling that is likely to offer geophysical novelties. This compels more development, one of the most urgent being probability the ability to define a geomagnetic field spectrum and to separate the sources at a regional scale as this would open new ways to characterize the magnetic field sources in the crust. This, we believe, is not necessarily a long call as the forthcoming abundance of magnetic field measurements and always denser compilations will prompt new interests and thus new practitioners in regional magnetic field modelling.

Acknowledgement We kindly thanks C. Beggan, V. Lesur and F. Simons for providing the data of Figs. 9.2 and 9.9 and helpful discussions and G. Plank for his helpful comments. For IPGP, this is contribution 2638.

References

Abramowitz M, Stegun A (1965) Handbook of mathematical functions. Dover, New York NY

Achache J, Abtout A, Le Mouël JL (1987) The downward continuation of Magsat crustal anomaly field over Southeast Asia. J Geophys Res 92(B11):11, 584–11, 596

Alldredge LR (1981) Rectangular harmonic analysis applied to the geomagnetic field. J Geophys Res 86(B4):3021–3026

Alldredge LR (1982) Geomagnetic local and regional harmonic analyses. J Geophys Res 87(B3):921–1926

Alldredge LR (1983) Varying geomagnetic anomalies and secular variation. J Geophys Res 88(B11):9443–9451

Backus G (1986) Poloidal and toroidal fields in geomagnetic field modelling. Rev Geophys 24(1):75–109

Backus G, Parker R, Constable C (1996) Foundations of geomagnetism. Cambridge University Press, Cambridge

Beggan C, Simons FJ (2009) Reconstruction of bandwidth-limited data on a sphere using Slepian functions: applications to crustal modelling. 505-TUE-1700-0728, IAGA Div.V, August, Sopron, Hungary

Chambodut A, Panet I, Mandea M, Diament M, Holschneider M, Jamet O (2005) Wavelet frames: an alternative to spherical harmonic representation of potential fields. Geophys J Int 163:875–899. doi:10.1111/j.1365-246X.2005.02754.x

Chapman S, Bartels J (1940) Geomagnetism. Oxford University Press, Oxford

Coddington EA (1955) Theory of ordinary differential equations. Mc Graw-Hill, New York, NY

Constable CG, Parker RL, Stark PB (1993). Geomagnetic field models incorporating frozen-flux constraints. Geophys J Int 113:419–433

Dautray R, Lions JL (1987, 1988) Analyse mathématique et calcul numérique pour les sciences et les techniques. Masson

De Santis A. (1991) Translated origin spherical cap harmonic analysis. Geophys J Int 106:253–263

De Santis A, Falcone C (1995) Spherical cap models of Laplacian potentials and general fields. In: Sanso F (ed) Geodetic theory today. Springer, New York, NY, pp 141–150

Freeden W, Glockner O, Thalhammer M (1999) Multiscale gravitational field recovery from GPS satellite-to-satellite tracking. Studia Geoph et Geod 43:229–264

Freeden W, Michel V (2000) Least-squares geopotential approximation by windowed Fourier transform and wavelet transform. In: Klees R, Haagmans R (eds) Wavelet geosciences. Springer, Berlin, pp 189–241

Friis-Christensen E, Lühr H, Hulot G (2006) SWARM: A constellation to study the Earth's magnetic field. Earth Planets Space 58:351–358

Gil A, Segura J, Temme NM (2009) Computing the conical function Pm−1/2+it(x). SIAM J Sci Comp 31(3): 1716–1741

Gillet N, Lesur V, Olsen N (2009) Geomagnetic core field secular variation models. Space Sci Rev pp 1–17, doi:10.1007/s11214-009-9586-6

Gonzalez-Velasco EA (1995) Fourier analysis and boundary value problems. Academic, Pacific Grove, CA

Haines GV (1985a) Spherical cap harmonic analysis. J Geophys Res 90(B3):2583–2591

Haines GV (1985b) Spherical cap harmonic analysis of geomagnetic secular variation over Canada 1960–1983. J Geophys Res 90(B14):12563–12574

Haines GV (1990) Modelling by series expansions: a discussion. J Geomagn Geoelectr 42:1037–1049

Hamoudi M, Thébault E, Lesur V, Mandea M (2007) GeoForschungsZentrum Anomaly Magnetic Map (GAMMA): A candidate model for the world digital magnetic anomaly map. Geochem Geophys Geosyst 8:Q06023. doi:10.1029/2007GC001638

Hobson EW (1965) The theory of spherical and ellipsoidal harmonics. Chelsea, New York, NY, second reprint edition

Holschneider M (1995) Wavelets: an analysis tool. Oxford mathematical monographs, Clarendon Press, Oxford

Holschneider M, Chambodut A, Mandea M (2003) From global to regional analysis of the magnetic field on the sphere using wavelets. Phys Earth Planet Inter 135. doi:10.1016/S0031-9201(02)00210-8

Howarth RJ (2001) A History of regression and related model-fitting in the earth sciences (1636–2000). Natl Resour Res 10(4):241–286

Jerri AJ (1998) The Gibbs phenomenon in Fourier analysis, splines and wavelet approximations. Kluwer, Dordrecht

Kellogg OD (1929) Foundations of potential theory. Dover, New York NY

Korhonen J, Fairhead D, Hamoudi M, Hemant K, Lesur V, Mandea M, Maus S, Purucker M, Ravat D, Sazonova T, Thébault E (2007) Magnetic anomalie map of the world/Carte des anomalies magnétiques du monde, 1st edn, 1:50,000,000, CCGM/CCGMW, ISBN 978-952-217-000-2

Langel RA, Estes RH, Mead GD, Fabiano EB, Lancaster ER (1980) Initial geomagnetic field model from MAGSAT vector data. Geophys Res Lett 7(10):793–796

Langel RA (1987) Main field. In: Jacobs JA (ed) Geomagnetism. pp 249–512. Academic, San Diego, CA

Langel RA, Sabaka TJ, Baldwin RT, Conrad JA (1996) The near-Earth magnetic field from magnetospheric and quiet-day ionospheric sources and how it is modelled. Phys Earth Planet Inter 98:235–267

Langel RA, Hinze WJ (1998) The magnetic field of the earth's lithosphere: the satellite perspective. Cambridge University Press, New York NY

Langlais B, Lesur V, Purucker ME, Connerney JEP, Mandea M (2009) Crustal magnetic field of terrestrial planets. Space Sci Rev. doi:10.1007/s11214-009-9557-y

Lesur V, Gubbins D (1999) Evaluation of fast spherical transforms for geophysical applications. Geophys J Int 139: 547–555

Lesur V (2006) Introducing localized constraints in global geomagnetic field modelling. Earth Planets Space 58:477–483

Lesur V, Maus S (2006) A global lithospheric magnetic field model with reduced noise level in the polar regions. Geophys Res Lett 33:L13304. doi:10.1029/2006GL025826

Lesur V, Wardinski I, Rother M, Mandea M (2008) GRIMM: the GFZ reference internal magnetic model based on vector satellite and observatory data. Geophys J Int 173:382–394. doi:10.1111/j.1365-246X.2008.03724.x

Lowes FJ (1999) Orthogonality and mean squares of vector fields given by spherical harmonic potentials. Geophys J Int 136:781–783

Maier T (2003) Multiscale geomagnetic field modelling from satellite data: theoretical aspects and numerical application. Unpublished PhD thesis, University of Kaiserslautern, Germany

Maier T, Mayer C (2003) Multiscale downward continuation of CHAMP FGM-data for crustal field modelling. In: Reigber C, Lühr H, Schwintzer P (eds) First CHAMP mission results for gravity, magnetic and atmospheric studies. Springer, Berlin, pp 288–295

Malin SRC, Düzgit Z, Baydemir N (1996) Rectangular harmonic analysis revisited. J Geophys Res 101(B12):28,205–28,209

Mandea M, Purucker ME (2005) Observing, modeling, and interpreting magnetic fields of the solid earth. Surv Geophys vol 26(4): pp. 415–459, doi:10.1007/s10712-005-3857-x

Maus S, Rother M, Hemant K, Stolle C, Lühr H, Kuvshinov A, Olsen N (2006) Earth's lithospheric magnetic field determined to spherical harmonic degree 90 from CHAMP satellite measurements. Geophys J Int 164:319–330. doi:10.1111/j.1365-246X.2005.02833.x

Maus S, Lühr H, Rother M, Hemant K, Balasis G, Ritter P, Stolle C (2007a) Fifth generation lithospheric magnetic field model from CHAMP satellite measurements. Geochem Geophys Geosyst 8:Q05013. doi:10.1029/2006GC001521

Maus S, Sazonova T, Hemant K, Fairhead JD, Ravat D (2007b) National geophysical data center candidate for the world digital magnetic anomaly map. Geochem Geophys Geosyst 8:Q06017. doi:10.1029/2007GC001643

Maus S, Yin F, Lühr H, Manoj C, Rother M, Rauberg J, Michaelis I, Stolle C, Müller RD (2008) Resolution of direction of oceanic magnetic lineations by the sixth-generation lithospheric magnetic field model from CHAMP satellite magnetic measurements. Geochem Geophys Geosyst 9:Q0702. doi:10.1029/2008GC001949

Maus S, Barckhausen U, Berkenbosch H, Bournas N, Brozena J, Childers V, Dostaler F, Fairhead JD, Finn C, von Frese RRB, Gaina C, Golynsky S, Kucks R, Lühr H, Milligan P, Mogren S, Müller RD, Olesen O, Pilkington M, Saltus R, Schreckenberger B, Thébault E, Caratori Tontini F (2009) EMAG2: A 2-arc min resolution earth magnetic anomaly grid compiled from satellite, airborne, and marine magnetic measurements. Geochem Geophys Geosyst 10:Q08005. doi:10.1029/2009GC002471

Maus S (2010) An ellipsoidal harmonic representation of Earth's lithospheric magnetic field to degree and order 720, Geochem. Geophys. Geosyst. 11:Q06015. doi:10.1029/2010GC003026

Mayer C, Maier T (2006) Separating inner and outer Earth's magnetic field from CHAMP satellite measurements by means of vector scaling functions and wavelets. Geophys J Int 167:1188–1203. doi:10.1111/j.1365-246X.2006.03199.x

Morse PM, Feshbach H (1953) Methods of theoretical physics. Mc Graw-Hill Company

Nakagawa I., Yukutake T (1985) Rectangular harmonic analyses of geomagnetic anomalies derived from MAGSAT data over the area of the Japanese Islands. J Geomagnetics. Geoelectric. 37(10):957–977

Nakagawa I, Yukutake T, Fukushima N (1985) Extraction of magnetic anomalies of crustal origin from Magsat over the area of the Japanese islands. J Geophys Res 90: 2609–2616

Olsen N, Holme R, Hulot G, Sabaka T, Neubert T, Toffner-Clausen L, Primdahl F, Jorgensen J, Leger J-M, Barraclough D, Bloxham J, Cain J, Constable C, Golovkov V, Jackson A, Kotze P, Langlais B, Macmillan S, Mandea M, Merayo J, Newitt L, Purucker M, Risbo T, Stampe M, Thomson A, Voorhies C (2000) ØRSTED initial field model. Geophys Res Lett 27(22):3607–3610

Olsen N, Lühr H, Sabaka TJ, Mandea M, Rother M, Tøffner-Clausen L, Choi S (2006) CHAOS—A Model of Earthś magnetic field derived from CHAMP, Ørsted, and SAC-C magnetic satellite data. Geophys J Int 166:67–75. doi:10.1111/j.1365-246X.2006.02959.x

Olsen N, Mandea M, Sabaka TJ, Tøffner-Clausen L (2009) CHAOS-2 A geomagnetic field model derived from one decade of continuous satellite data. Geophys J Int 179: 1477–1487. doi:10.1111/j.1365-246X.2009.04386.x

Olver FWJ. (1997) Asymptotics and special functions. Peters AK, Natick, Massachusetts

Panet I, Chambodut A, Diament M, Holschneider M, Jamet O (2006) New insights on intraplate volcanism in French Polynesia from wavelet analysis of GRACE, CHAMP, and sea surface data. Geophys J Res 111:B09403. doi:10.1029/2005JB004141

Purucker ME, Whaler W (2007) Crustal magnetism. : In: Kono M (ed) Geomagnetism, Elsevier, Amsterdam, treatise on geophysics, Chapter 6, vol 5. pp 195–237

Reddy, BD (1998) Introductory functional analysis, vol 27. Springer, New York, NY, Texts in applied mathematics

Reigber C, Lühr H, Schwintzer P (2002) CHAMP Mission status. Adv Space Res 30(2), 129–134. doi:10.1016/S0273-1177(02)00276-4

Robin L (1958) Fonctions sphériques de Legendre et fonctions sphéroidales, vol II and III. Gauthier-Villars, Paris

Sabaka TJ, Baldwin RT (1993) Modeling the Sq magnetic field from POGO and MAGSAT satellite and contemporaneous hourly observatory data: Phase I. Contract Report HSTX/G&G9302

Sabaka TJ, Olsen N, Purucker ME (2004) Extending comprehensive models of the Earth's magnetic field with Ørsted and CHAMP data. Geophys J Int 159:521–547. doi:10.1111/j.1365–246X.2004.02421.x

Sabaka TJ, Olsen N (2006) Enhancing comprehensive inversions using the SWARM constellation. Earth Planet Space 58: 371–395

Sabaka TJ, Hulot G, Olsen N (2009) Mathematical properties relevant to geomagnetic field modelling. In: Freeden W, Nashed Z, Sonar T (eds) Handbook of Geomathematics. Springer, Heidelberg, (in press), ISBN 978-3-642-01547-2

Shure L, Parker RL, Backus GE (1982) Harmonic splines for geomagnetic modelling. Phys Earth Planet Inter 28: 215–229

Simons FJ, Dahlen FA (2006) Spherical slepian functions and the polar gap in geodesy. Geophys J Int 166:1039–1061. doi: 10.1111/j.1365-246X.2006.03065.x

Simons FJ, Dahlen FA, Wieczorek MA (2006) Spatiospectral concentration on a sphere. SIAM Rev 48(3):504–536. doi: 10.1137/S0036144504445765

Simons FJ, Hawthorne JC, Beggan CD (2009) Efficient analysis and representation of geophysical processes using localized spherical basis functions. In: Goyal VK, Papadakis M, Van de Ville D (eds) Wavelets XIII. 7446:74460G1-15. doi:10.1117/12.825730

Simons FJ (2010) Slepian functions and their use in signal estimation and spectral analysis. In: Freeden W, Nashed Z, Sonar T (eds) Handbook of geomathematics. Springer, Heidelberg, (in press), ISBN: 978-3-642-01547-2

Stockman R, Finlay CC, Jackson A (2009) Imaging Earth's crustal magnetic field with satellite data: a regularized spherical triangle tessellation approach. Geophys J Int 179: 929–944. doi:10.1111/j.1365-246X.2009.04345.x

Sneeuw N (1994) Global spherical harmonic analysis by least-squares and numerical quadrature methods in historical perspective. Geophys J Int 118:707–716

Thébault E, Schott JJ, Mandea M, Hoffbeck JP (2004) A new proposal for spherical cap harmonic analysis. Geophys J Int 159:83–105

Thébault E (2006) Global lithospheric magnetic field modeling by successive regional analysis. Earth Planets Space 58: 485–495

Thébault E, Schott JJ, Mandea M, (2006a) Revised spherical cap harmonic analysis (RSCHA): validation and properties. J Geophys Res 111:B01102. doi:10.1029/2005JB003836

Thébault E, Mandea M, Schott JJ (2006b) Modelling the lithospheric magnetic field over France by means of revised spherical cap harmonic analysis (R-SCHA). J Geophys Res 111:B05102. doi:10.1029/2005JB004110

Thébault E (2008) A proposal for regional modelling at the Earth's surface, R-SCHA2D. Geophys J Int. doi:10.1111/j.1365-246X.2008.03823.x

Thébault E, Gaya-Piqué L (2008) Applied comparisons between SCHA and R-SCHA regional modelling techniques. Geochem Geophys Geosyst 9:Q07005. doi:10.1029/2008GC001953

Thébault E, Purucker ME, Whaler K, Langlais B, Sabaka TJ (2010) The Magnetic field of the Earth's lithosphere. Space Sci Rev, doi:10.1007/S11214-010-9667-6

Torta JM, Gaya-Piqué LR, De Santis A (2006) Spherical cap harmonic analysis of the geomagnetic field with application for aeronautical mapping. In: Rasson JL, Delipetrov T (eds) Geomagnetics for aeronautical safety: a case study in and around the balkans. Springer, Dordrecht, pp 291–307